



# MARSOL

## Demonstrating Managed Aquifer Recharge as a Solution to Water Scarcity and Drought

### Hydrogeological modelling at the South Portugal MARSOL demonstration sites

<b>Deliverable No.</b>	D4.4
<b>Version</b>	1.0
<b>Version Date</b>	13.07.2016
<b>Author(s)</b>	J.P. Lobo Ferreira, Teresa E. Leitão, Manuel M. Oliveira, Tiago Martins, Rogério Mota (all LNEC, besides the cooperation of Ana Maria Carmen from University of Ferrara) (LNEC) José Paulo Monteiro, Luís R.D. Costa, Rui Hugman (UAAlg) Tiago Carvalho, Rita Carvalho, Raquel Sousa (TARH)
<b>Dissemination Level</b>	PU
<b>Status</b>	Final



The MARSOL project has received funding from the European Union's Seventh Framework Programme for Research, Technological Development and Demonstration under grant agreement no 619120.



## Contents

<b>1.</b>	<b>INTRODUCTION AND MAIN GOALS .....</b>	<b>9</b>
<b>2.</b>	<b>MARSOL DEMO SITE 2: ALGARVE AND ALENTEJO, SOUTH PORTUGAL .....</b>	<b>11</b>
<b>2.1</b>	<b>PT1: Rio Seco and Campina de Faro aquifer system (Algarve).....</b>	<b>11</b>
2.1.1	Introduction and objective .....	11
2.1.2	Water balances.....	14
2.1.3	Infrastructures for MAR .....	20
2.1.4	Water origin for MAR (water budget) .....	22
2.1.5	Numerical groundwater flow and transport model for Campina de Faro aquifer.....	24
<b>2.2</b>	<b>PT2: Querença-Silves limestone karstic aquifer system (Algarve) .....</b>	<b>29</b>
2.2.1	Introduction and objective .....	29
2.2.2	Water balances.....	40
2.2.3	Infrastructures for MAR .....	41
2.2.4	Water origin for MAR (water budget) .....	42
2.2.5	Numerical groundwater flow model for Querença-Silves aquifer .....	43
2.2.6	Numerical modelling of soil-column experiments at LNEC.....	52
<b>2.3</b>	<b>PT3: Melides aquifer, river and lagoon (Alentejo).....</b>	<b>62</b>
2.3.1	LNEC physical sandbox model .....	62
2.3.2	Investigation experiments and monitoring .....	63
	<b>REFERENCES.....</b>	<b>64</b>

## Figures

Figure 1 – PT MARSOL DEMO sites location (the aquifers boundaries are marked in grey) .....	9
Figure 2 – Campina de Faro N-S hydrogeological section (Stigter, 2005) .....	11
Figure 3 – Campina de Faro hydrogeological model, presented in JK15 well log (Silva <i>et al.</i> , 1986) ...	12
Figure 4 – Evolution of the Nitrate contamination from 1995 until May 2014 .....	13
Figure 5 – Distribution of recharge in the Campina de Faro aquifer system (Lobo Ferreira <i>et al.</i> , 2006) .....	14
Figure 6 – Yearly variation of the modelled parameters (including aquifer recharge) in the artificial recharge area in an alluvium soil (Soil = “Atac”) and in a regosol (Soil = “Rgc”) (Lobo Ferreira <i>et al.</i> , 2006).....	15
Figure 7 – River flow cumulative curve and infiltration capacity of the IB (depending on the area of the IB), considering the infiltration capacity = 1.2 m/d .....	15
Figure 8 – Monthly rainfall and reference evapotranspiration (ET <sub>o</sub> ) fluctuation for the period 10/2001-09/2014 in São Brás de Alportel meteorological station .....	16
Figure 9 – Yearly rainfall and reference evapotranspiration (ET <sub>o</sub> ) fluctuation for the period 10/2001- 09/2014 in São Brás de Alportel meteorological station .....	17
Figure 10 – Monthly surface runoff, natural recharge and actual evapotranspiration fluctuation for the period 10/2001-09/2014 in Rio Seco hydrographic basin upstream the infiltration basins .....	17
Figure 11 – Yearly surface runoff, natural recharge and actual evapotranspiration fluctuation for the period 10/2001-09/2014 in Rio Seco hydrographic basin upstream the infiltration basins.....	18
Figure 12 – Average surface runoff distribution in Rio Seco hydrographic basin upstream the infiltration basins.....	18
Figure 13 – Average groundwater recharge distribution in Rio Seco hydrographic basin upstream the infiltration basins.....	19
Figure 14 – Average actual evapotranspiration distribution in Rio Seco hydrographic basin upstream the infiltration basins .....	19
Figure 15 – Hydrograph basin above Rio Seco MAR facilities and groundwater bodies .....	20
Figure 16 – Intensive greenhouse agricultural activity in the Campina de Faro aquifer system and traditional system of drains for collection of rainwater .....	22
Figure 17 – Traditional large diameter wells potentially suited for injection of harvested water .....	22
Figure 18 – Top: 32 year average annual rainfall spatial distribution on Campina de Faro aquifer system (CFAS) (based on Nicolau, 2002) and greenhouse’s locations (based on APA-ARH Algarve,	



unpublished). Bottom left: 32 year average monthly and annual rainfall distribution values for the CFAS (based on Nicolau, 2002).....	23
Figure 19 – Vertical structure of the 3D Campina de Faro aquifer model .....	25
Figure 20 – Observed (top) nitrate concentration and simulated nitrated contamination after calibration of flow and mass-transport model parameters .....	27
Figure 21 – Cross-section view of the CF showing nitrate concentration without (top) and with (bottom) the injection of 1.63 hm <sup>3</sup> /year in large wells.....	28
Figure 22 – 3D view of the nitrate contamination plume at CF without (left) and with (right) the injection of 1.63 hm <sup>3</sup> /year in large wells .....	28
Figure 23 – Querença-Silves aquifer system’s geology. Underlined features are the ones identified within the aquifer limits. Almeida <i>et al.</i> (2000) .....	30
Figure 24 – Geometry of the carbonated rocks of early Jurassic which constitute the most important support of the aquifer system Querença-Silves (dark blue colour, to the left of the Algibre thrust). Adapted from Manuppella <i>et al.</i> (1993) .....	30
Figure 25 – Site location along Ribeiro Meirinho stream and central-western area of Querença-Silves aquifer and its piezometry (upper right: modelled; lower right: measured) (Leitão <i>et al.</i> , 2014) .....	31
Figure 26 – Geophysical field word in 2014. Processing data on site .....	32
Figure 27 - Geophysical field word in 2016. Portuguese MARSOL team .....	33
Figure 28 - Location of 2014 geophysical profiles in Querença-Silves aquifer at Cerro do Bardo site .	34
Figure 29 - Geophysical surveys (absolute (reference) and % change) in Querença-Silves aquifer at Cerro do Bardo performed during the injection tracer test of 2014 - results from profile P1 .....	34
Figure 30 - Geophysical surveys (absolute (reference) and % change) in Querença-Silves aquifer at Cerro do Bardo performed during the injection tracer test of 2014 - results from profile P2 .....	35
Figure 31 - Geophysical surveys (absolute (reference) and % change) in Querença-Silves aquifer at Cerro do Bardo performed during the injection tracer test of 2014 - results from profile P3 .....	35
Figure 32 – Location of 2014 and 2016 geophysical profiles in Querença-Silves aquifer at Cerro do Bardo site .....	36
Figure 33 - Geophysical surveys (absolute (reference) and % change) in Querença-Silves aquifer at Cerro do Bardo performed during the large injection tracer test of 2016 - results from profile P1 ....	37
Figure 34 - Geophysical surveys (absolute (reference) and % change) in Querença-Silves aquifer at Cerro do Bardo performed during the large injection tracer test of 2016 - results from profile P2 ....	38
Figure 35 – Location and main supply wells in Querença-Silves aquifer system.....	40

Figure 36 – Average Querença-Silves aquifer recharge (period 1941-1991) (source: Oliveira <i>et al.</i> 2008).....	41
Figure 37 – Hydrograph basin above selected MAR facilities in PT2 and related groundwater bodies	42
Figure 38 – Development of the 3D geometrical mesh of the Querença-Silves aquifer model .....	44
Figure 39 – Average Querença-Silves aquifer recharge (period 1941-1991) as calculated by Oliveira <i>et al.</i> (2011) .....	44
Figure 40 – Observed and simulated hydraulic head at several observation wells used to calibrate and validate the Querença–Silves numerical flow model for the 2D and 3D geometry .....	45
Figure 41 – Numerical model calibrated hydraulic conductivity distribution and location of Dirichlet boundary conditions and well .....	46
Figure 42 – Residual between hydraulic head without and with injection of 10 hm <sup>3</sup> /year .....	47
Figure 43 – Sharp interface analysis of saltwater-freshwater interface at Querença-Silves. ....	48
Figure 44 – Residual between hydraulic head without and with injection of 3 hm <sup>3</sup> /year .....	49
Figure 45 – LEFT: Records for water displacement in the well as a function of time. RIGHT: Scatter plot between hydraulic load and infiltration rate and its linear fits .....	50
Figure 46 – Effect of mesh density on simulated hydraulic head during injection test.....	51
Figure 47 – Comparison of observed and calculated data based on optimized values of aquifer parameters .....	52
Figure 48 – Soil-column apparatus and diagram of operation.....	53
Figure 49 – Nitrogen cycle components concentration in Column 3 inflow/outflow.....	55
Figure 50 – Nitrogen cycle components concentration in Column 4 inflow/outflow.....	55
Figure 51 – Hydrus-1D results for nitrogen simulation (concentration through depth) .....	57
Figure 52 – Hydrus-1D results for nitrogen simulation for node 1 and 2 (S1 – ammonia, S2 – nitrites, S3 – nitrates) .....	59
Figure 53 – Hydrus-1D results for nitrogen simulation for nodes 3, 4 and 5 (S1 – ammonia, S2 – nitrites, S3 – nitrates) .....	60
Figure 54 – LNEC Physical (sandbox) model construction .....	62
Figure 55 – LNEC physical (sandbox) model sections, A, B and C .....	62
Figure 56 – Schematic diagram of the physical (sandbox) model dimensions .....	63

## Tables

Table 1 – Groundwater bodies intersected by the hydrographic basin above Rio Seco MAR facilities	20
Table 2 – Estimated average monthly and annual potential rainfall harvested from greenhouses.....	24
Table 3 – Summary of the 2014’ geophysical survey .....	32
Table 4 – Summary of the 2016’ geophysical survey .....	33
Table 5 – Abstraction volumes per category for scenario 1 and 2.....	47
Table 6 – Results of the recovery period from the injection test. Water displacement and infiltration rate .....	50
Table 7 – Synthesis of the operating details of the soil-column experiments conducted in the natural soil .....	54
Table 8 – Input data for Hydrus-1D C3 and C4 models. ....	56



## 1. INTRODUCTION AND MAIN GOALS

The main objectives of WP4 “DEMO Site 2: Algarve and Alentejo, South Portugal” are to demonstrate how MAR can contribute as an alternative source of water, in the context of an integrated and inter-annual water resources management, as well as in solving groundwater quality problems caused by previous agricultural practices and wastewater discharges.

Three DEMO sites (Figure 1) have been chosen for WP4:

- PT1: Rio Seco and Campina de Faro aquifer system (Algarve)
- PT2: Querença-Silves limestone karstic aquifer system (Algarve)
- PT3: Melides aquifer, river and lagoon (Alentejo)

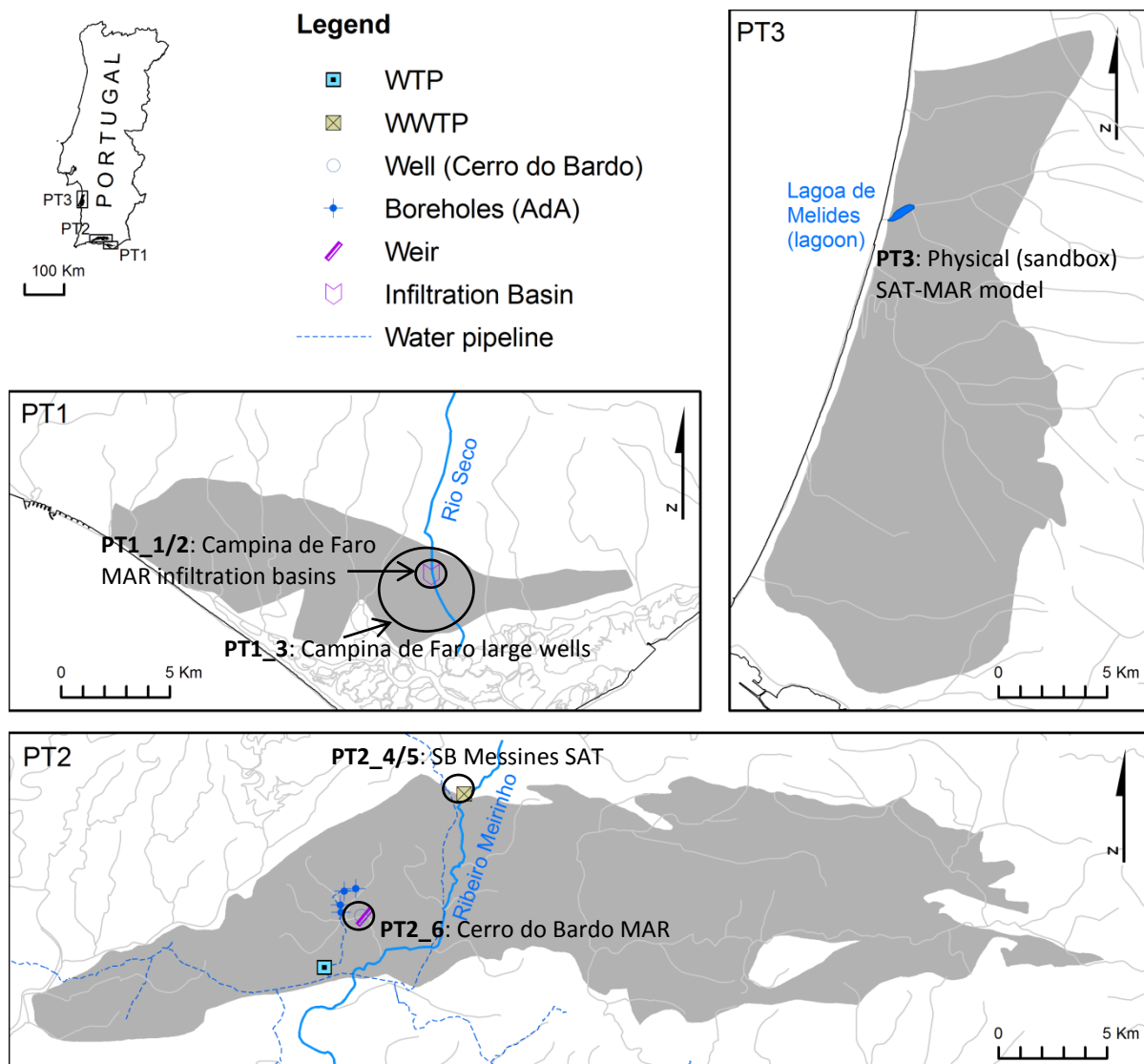


Figure 1 – PT MARSOL DEMO sites location (the aquifers boundaries are marked in grey)

In PT1 – Rio Seco and Campina de Faro aquifer system (Algarve) – the main goal is to improve the groundwater quality heavily contaminated with nitrates (vulnerable zone), mainly due to agriculture bad practices.

In PT2 – Querença-Silves limestone karstic aquifer system (Algarve) – there are two main sub-areas and two goals: (1) develop a soil-aquifer-treatment (SAT) system to improve the water quality of treated effluents from a waste water treatment plant (WWTP) (PT2\_4), which discharges into Ribeiro Meirinho river (PT2\_5) that recharges the karstic aquifer, and (2) increase groundwater storage at Cerro do Bardo karstic area using wet years surface water surplus to increase the water availability in dry years and facilitate downstream water supply.

In PT3 – Melides aquifer, river and lagoon (Alentejo) – the main goal is to use SAT-MAR to remove rice field pollutants prior to their discharge in Melides lagoon.

The work developed for the different DEMO sites was developed in the following tasks:

- Task 4.1: Recharge water availability
- Task 4.2: Developing the (MAR) infrastructures
- Task 4.3: Investigation and monitoring
- Task 4.4: Modelling

The results are being presented in five main deliverables:

- D4.1: Water sources and availability at the South Portugal MARSOL demonstration sites
- D4.2: South Portugal MARSOL demonstration sites characterisation
- D4.3: Monitoring results from the South Portugal MARSOL demonstration sites
- D4.4: Hydrogeological modelling at the South Portugal MARSOL demonstration sites
- D4.5: MAR to improve the groundwater status in South Portugal (Algarve and Alentejo)

This report presents the results from D4.4: Hydrogeological modelling at the South Portugal MARSOL demonstration sites.

## 2. MARSOL DEMO SITE 2: ALGARVE AND ALENTEJO, SOUTH PORTUGAL

### 2.1 PT1: RIO SECO AND CAMPINA DE FARO AQUIFER SYSTEM (ALGARVE)

#### 2.1.1 Introduction and objective

##### Conceptual model

The conceptual model of the Campina de Faro aquifer system is detailed on Deliverable 4.2 from where this text was withdrawn. Figure 2 (Stigter, 2005) presents a hydrogeological section of Campina de Faro area. The oldest formations belong to the Jurassic gypsiferous material that locally outcrops near Faro and is related to diapiric activity.

According to Stigter (2005), the oldest aquifer system that occurs in the Campina de Faro area is the Cretaceous, formed by limestone layers separated by marls (Figure 2). They dip to the south (20°-30°) and crop out in the NW part of the area. The top of the sediments is found at a depth below 200 m, near the city of Faro (Stigter, 2000). According to Manupella (1992, *in* Stigter, 2005) the thickness of Cretaceous aquifer is larger than 1000 m. A grabben-like structure was formed at the end of the Cretaceous where Miocene limestones and, later, sands and marls were deposited in discordance (Silva, 1988, *in* Stigter, 2000).

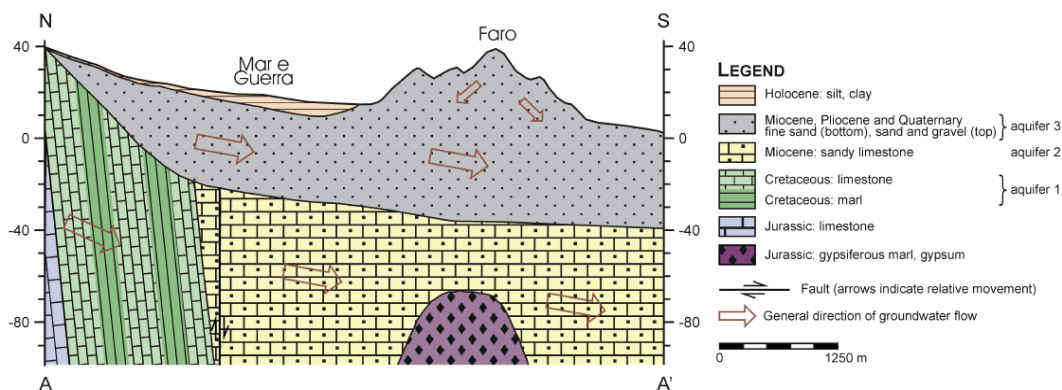


**Figure 2 – Campina de Faro N-S hydrogeological section (Stigter, 2005)**

Miocene fossil-rich sandy-limestone deposits constitute the second aquifer. It deepens to the East but, because of the presence of several N-S faults, a stepwise structure is present (Silva *et al.*, 1986 and Silva, 1988, *in* Stigter, 2000). There are few outcrops of Miocene limestones in Campina de Faro, also because they are covered by fine sand deposited during Miocene. The depth of the top of Miocene formations varies between 3 and 25 m below surface and the presence of marls seems to be very irregular (Silva, 1988 *in* Stigter, 2000). The topography of the top of the Miocene is irregular. Despite Miocene outcrops are very few and small, Miocene formations thickness is very large. It increases from north to south and exceeds 200 m near the coast. According to Antunes and Pais (1987, *in* INAG, 2000) a deformation might have affected the Miocene deposits and that could explain the apparent thicknesses, larger than the real ones. The carbonated fraction varies from 60% to 95% with a decreasing trend from the base to the top (Silva, 1988).

Covering the Miocene deposits, sands, clayey sandstones, gravels and conglomerates of the Plio-Quaternary are found (“Areias e Cascalheiras de Faro-Quarteira” formation), with a thickness very variable. They crop in the NW and also near the city of Faro. Stigter (2000) refers that its thickness varies between 8 and 50 m. According to Moura and Boski (1994, in INAG, 2000) this formation has a maximum thickness of 30 m. Silva (1998, in INAG, 2000) refers that the thickness of these deposits can reach, in some places, a thickness of 60 m.

The third aquifer system is formed by the fine sand of Miocene and also the Plio-Quaternary sand and gravels. This aquifer presents an average thickness of 50 m (Stigter, 2004). Despite being partly covered by Holocenic materials, this aquifer is still considered phreatic, because their thickness is often too small to give confined characteristics to the underlying aquifer. According to Silva (1988) the average thickness of this aquifer is 25 m, but reaching maximum values of 60 m and 65 m near Galvana and in Quinta do Lago, respectively.

Some authors refer the existence of a confining layer between the second and the third aquifers. According to Silva *et al.* (1986), that separation is made by several silty-clayey-sandy layers (Figure 3) with variable thickness and apparently with some lateral continuity. Nevertheless, one cannot exclude the possibility of some hydraulic connection in sectors where that confining layers are absent (INAG, 2000).

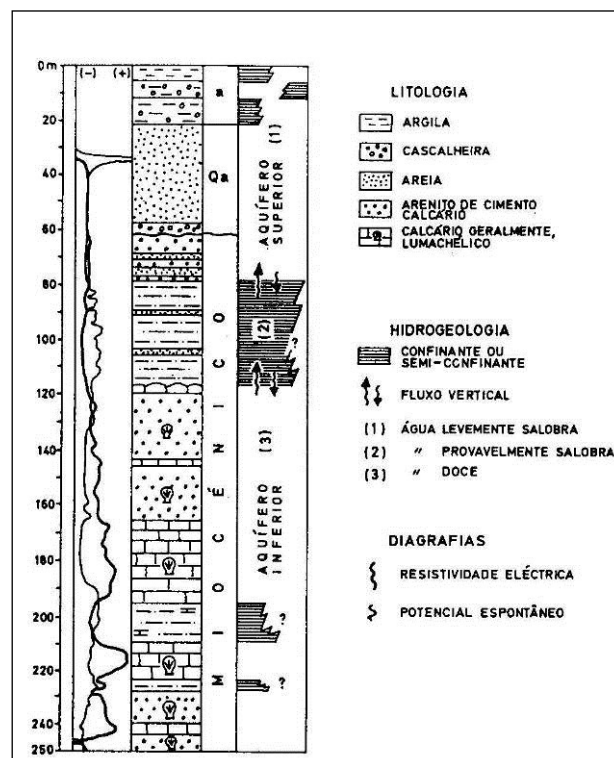


Figure 3 – Campina de Faro hydrogeological model, presented in JK15 well log (Silva *et al.*, 1986)

Furthermore, in some situations there is a hydraulic connection artificially established due to new wells built within old large wells with the aim of extracting water from the Miocene and confined aquifer. This connection facilitates the confined aquifer contamination coming from the overlying phreatic aquifer.



According to Stigter (2005), the general direction of groundwater flow is N-S (cf. Figure 2). There are preferential flow paths formed by the N-S trending faults but the NW-SE trending fault acts like a barrier, which is indicated by the steeper hydraulic gradient of the water table in the north.

### Modelling context

A 3D finite element flow and transport model of the Campina de Faro aquifer (CF) (MARSOL Portuguese case study PT1), was developed in order to analyse the nitrate's plume evolution on this system and how can MAR contribute to improve the aquifer water quality.

The nitrate contamination in Campina de Faro aquifer is an issue that has been raising a relevant awareness among the water authorities and end users in Algarve and it has been the target of several studies since the 2000's (e.g. Stigter *et al.*, 2006a; Stigter *et al.*, 2006b; Stigter *et al.*, 2008; Diamantino Roseiro 2009; Stigter *et al.*, 2013). During MARSOL project, at Campina de Faro aquifer case study, the model is intended to show MAR can be a reliable solution to contribute to the flushing of the nitrate contamination towards the coast. The evolution of nitrate plume contamination at Campina de Faro is shown in Figure 4.

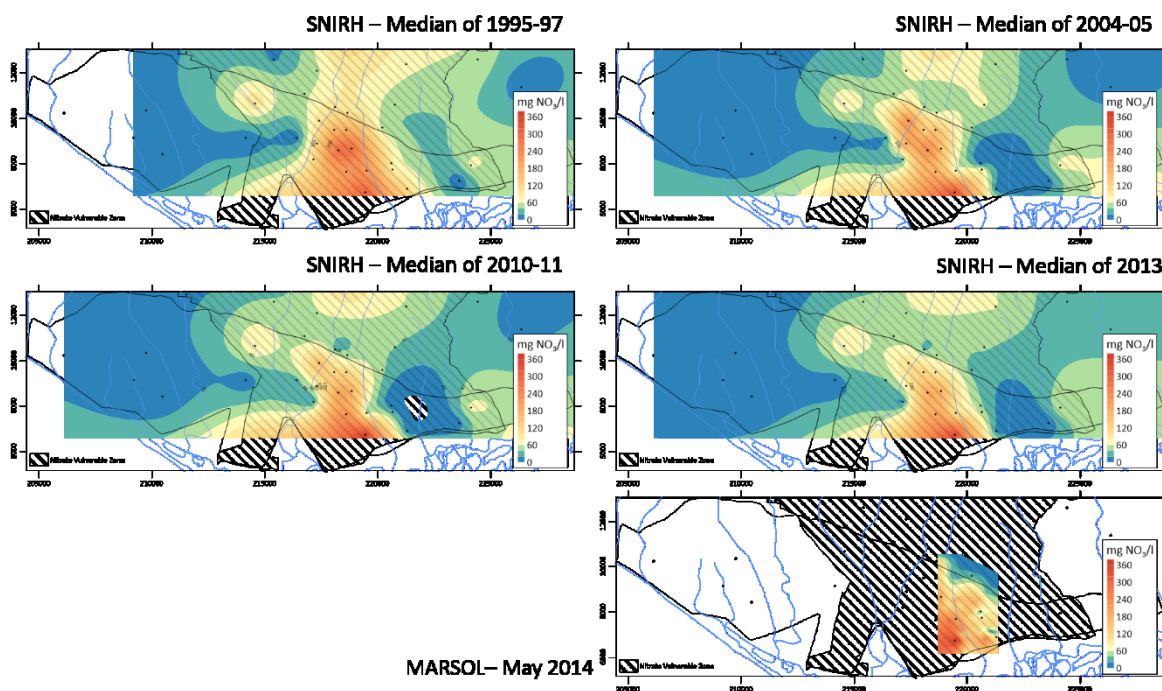


**Figure 4 – Evolution of the Nitrate contamination from 1995 until May 2014**

Nitrate intake at Campina de Faro aquifer is a subject which has been thoroughly studied at University of Algarve (Stigter *et al.*, 2006a; Stigter *et al.*, 2008; Stigter *et al.*, 2013).

According to Stigter *et al.* (2013) annual nitrate requirements are 200-300 kg/ha for the crops grown in the area and for this study an average nitrate loss of 20% to the groundwater is considered, resulting in an annual intake of 63.4 ton. However, this value may have been considerably higher in the past. An additional contribution of 50 mgNO<sub>3</sub>/L caused by the irrigation return flow (Stigter *et al.* 2006a) is considered and implemented in the model, which corresponds to 114 ton/yr. Contributions from other sources were not included.

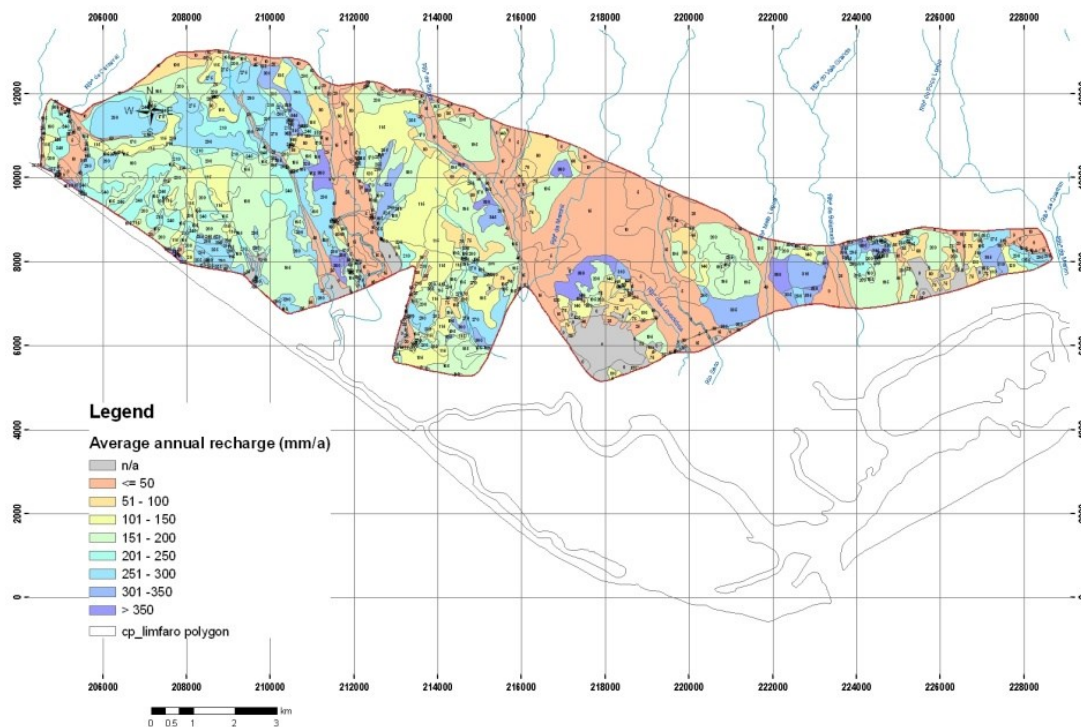
## 2.1.2 Water balances

### Natural recharge

Recharge values for the study area were calculated by Lobo-Ferreira *et al.* (2006) based on the FAO dual crop coefficient method using a sequential daily water balance model (BALSEQ\_MOD) developed by Oliveira (2004). This model encompasses as input data: daily precipitation, monthly reference evapotranspiration, root depths (time dependent), extent of land occupation, soil wilting point, soil field capacity, soil porosity, soil hydraulic conductivity, soil top horizon material and soil initial water content. Recharge is estimated as deep infiltration = precipitation – direct surface runoff – real evapotranspiration – variation of soil water content (Lobo-Ferreira *et al.*, 2006).

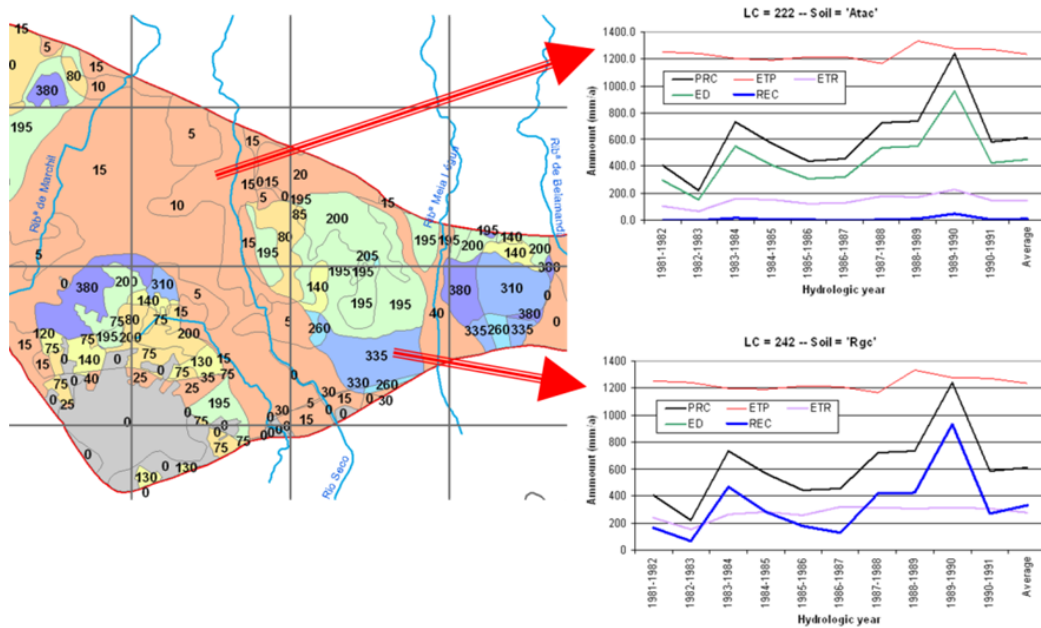
Average aquifer recharge in The Campina de Faro aquifer system was estimated in Lobo-Ferreira *et al.* (2006) as 139 mm/year, 23% of the precipitation, despite, depending on the land use and the soil properties, the recharge distribution is highly variable. Lower values are in the order of 5 mm/year in the alluvium formations and larger values can go up to 380 mm/year in sandy outcrops

Figure 5 shows the average annual recharge for the Campina de Faro aquifer accordingly to Lobo-Ferreira *et al.* (2006).



**Figure 5 – Distribution of recharge in the Campina de Faro aquifer system (Lobo Ferreira *et al.*, 2006)**

For instance Figure 6 shows the recharge distribution along the years in these types of soil/land use combinations.



**Figure 6 – Yearly variation of the modelled parameters (including aquifer recharge) in the artificial recharge area in an alluvium soil (Soil = “Atac”) and in a regosol (Soil = “Rgc”) (Lobo Ferreira *et al.*, 2006)**

**Rio Seco hydrographic basin upstream the infiltration basins**

A study for the estimation of water available for infiltration under natural conditions was developed using 10 year daily data from Rio Seco station (Figure 7).

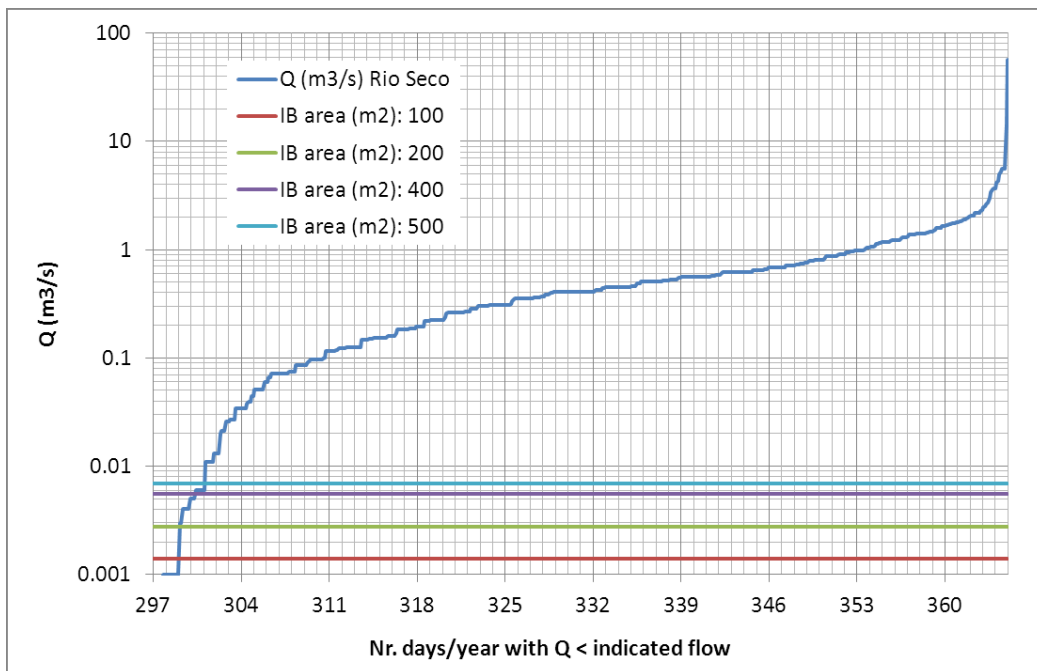


**Figure 7 – River flow cumulative curve and infiltration capacity of the IB (depending on the area of the IB), considering the infiltration capacity = 1.2 m/d**

Estimation of the relation between infiltration capacity of the IB and river surface flow (Figure 7) determining the average number of days per year in which river flow is higher than the infiltration capacity of the IB. The value of 200 m<sup>2</sup> corresponds to the old existing IB and the value 400 m<sup>2</sup> corresponds to the actually existing infiltration basins capacity.

The BALSEQ\_MOD model was also run for the area of the hydrographic basin upstream Rio Seco river infiltration basins in order to determine the available amount of water for the infiltration basins. The period of analysis is of 13 years, from 1/10/2001 until 30/9/2014. Precipitation was taken from the meteorological gauge station 31J/01C – São Brás de Alportel belonging to the Portuguese Environment Agency (data accessible from <http://snirh.pt/index.php?idMain=2&idItem=1>) that collected reliable data until 31/05/2009. Lacking data was estimated using other rain gauge stations, namely in first place 31J/04UG – Estói, also from the Portuguese Environment Agency, and, in second place, the meteorological station of Patação, belonging to the Algarve Regional Directorate of Agriculture and Fisheries with data starting from 01-01-2006 (<http://www.drapalg.min-agricultura.pt/ema/pat.htm>). The relation of average precipitations in these stations was used to fill the gaps.

Daily reference evapotranspiration (ET<sub>o</sub>) was estimated using the FAO Penman-Monteith method with data of daily maximum and minimum temperature, daily average relative humidity or hourly relative humidity, daily solar radiation, and daily wind speed, also measured in the meteorological gauge station 31J/01C – São Brás de Alportel. Missing data was estimated by several procedures using measurements in the 30K/02C – Picota meteorological station, also from the Portuguese Environment Agency, and, in second place, using data registered in the above mentioned meteorological station of Patação.

Average yearly precipitation and average yearly reference evapotranspiration were estimated in São Brás de Alportel meteorological station as 638 mm/year and 1023 mm/year, with the monthly and yearly distributions shown in Figure 8 and Figure 9, respectively.

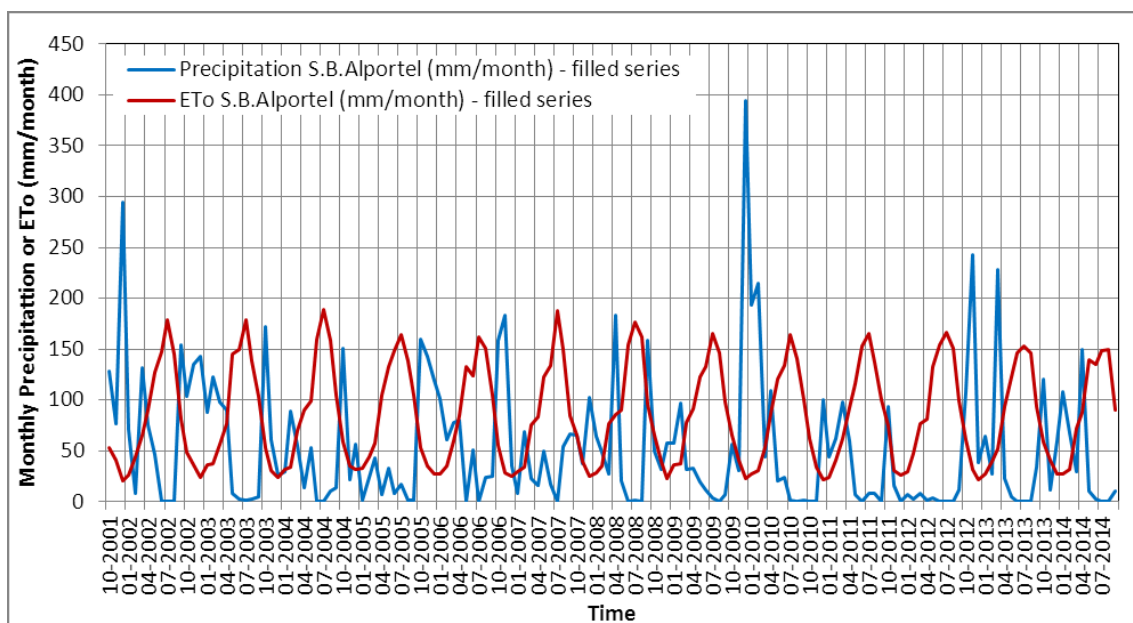


**Figure 8 – Monthly rainfall and reference evapotranspiration (ET<sub>o</sub>) fluctuation for the period 10/2001-09/2014 in São Brás de Alportel meteorological station**

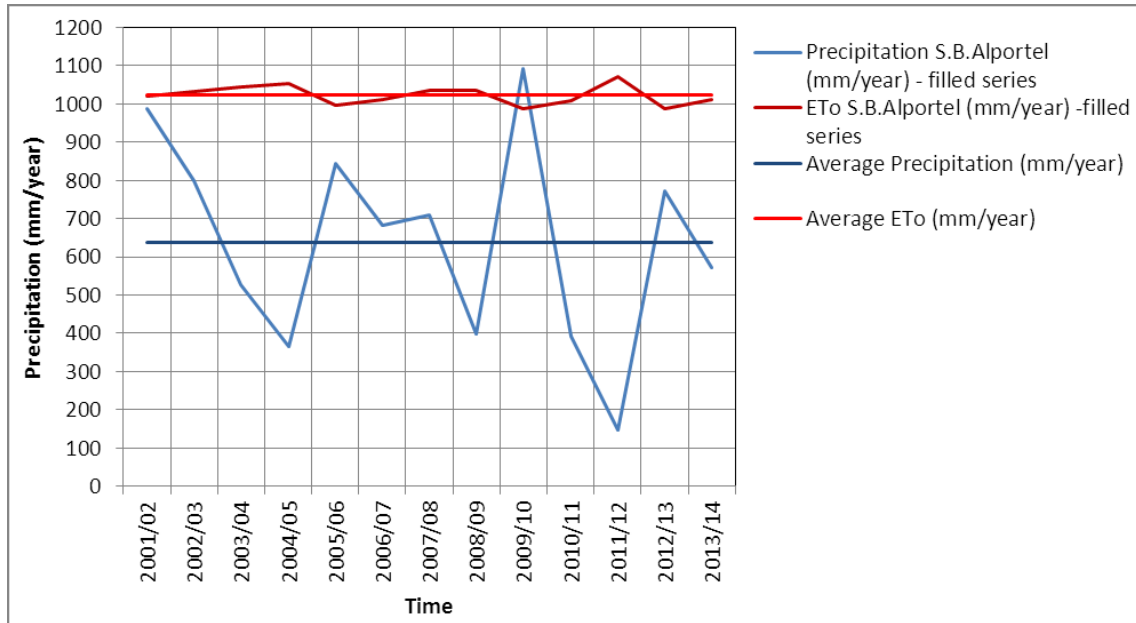


**Figure 9 – Yearly rainfall and reference evapotranspiration (ETo) fluctuation for the period 10/2001-09/2014 in São Brás de Alportel meteorological station**

Information on soil parameters and land use was taken from the Soil Map of Portugal at the 1:50000 scale from IHERA and from 1:100000 scale 2006-Corine Land Cover (Caetano *et al.*, 2009).

The results obtained by the BALSEQ\_MOD model may be summarised as follows: average surface runoff = 360 mm/year; average groundwater recharge = 28 mm/year; average actual evapotranspiration = 250 mm/year. The average monthly and yearly distribution of the values is represented in Figure 10 and Figure 11.

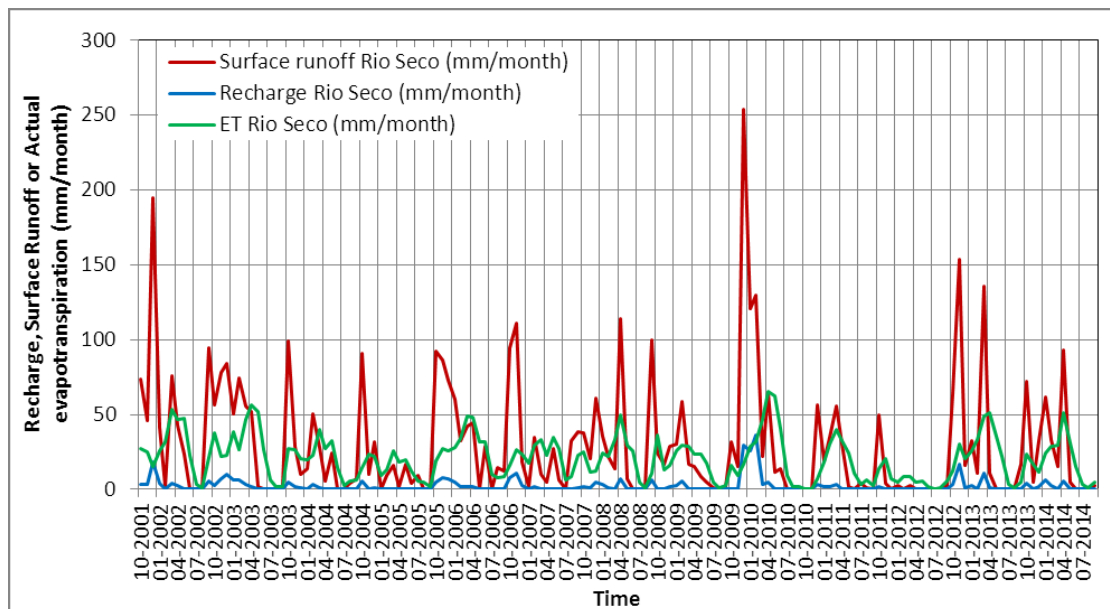


**Figure 10 – Monthly surface runoff, natural recharge and actual evapotranspiration fluctuation for the period 10/2001-09/2014 in Rio Seco hydrographic basin upstream the infiltration basins**





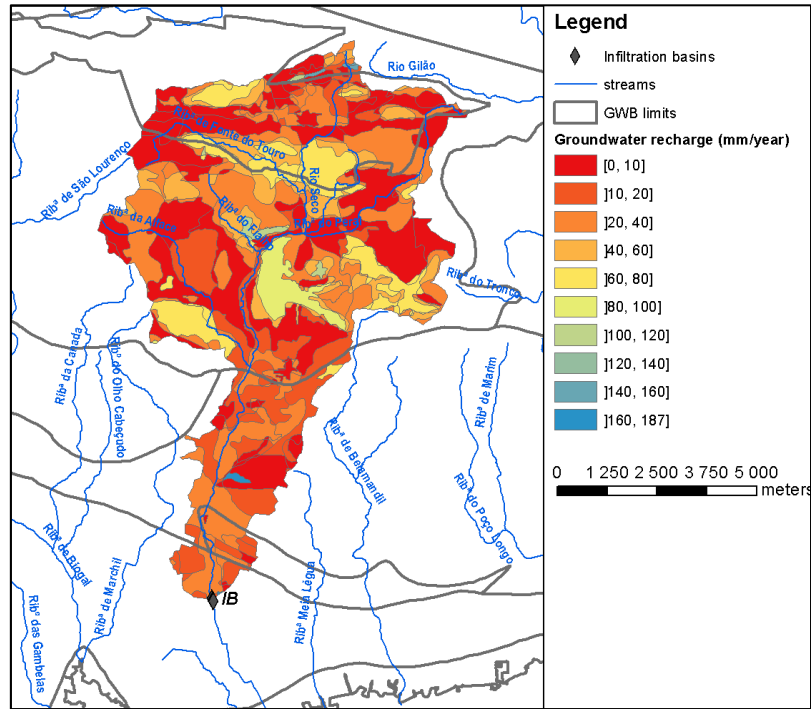


Figure 13 – Average groundwater recharge distribution in Rio Seco hydrographic basin upstream the infiltration basins

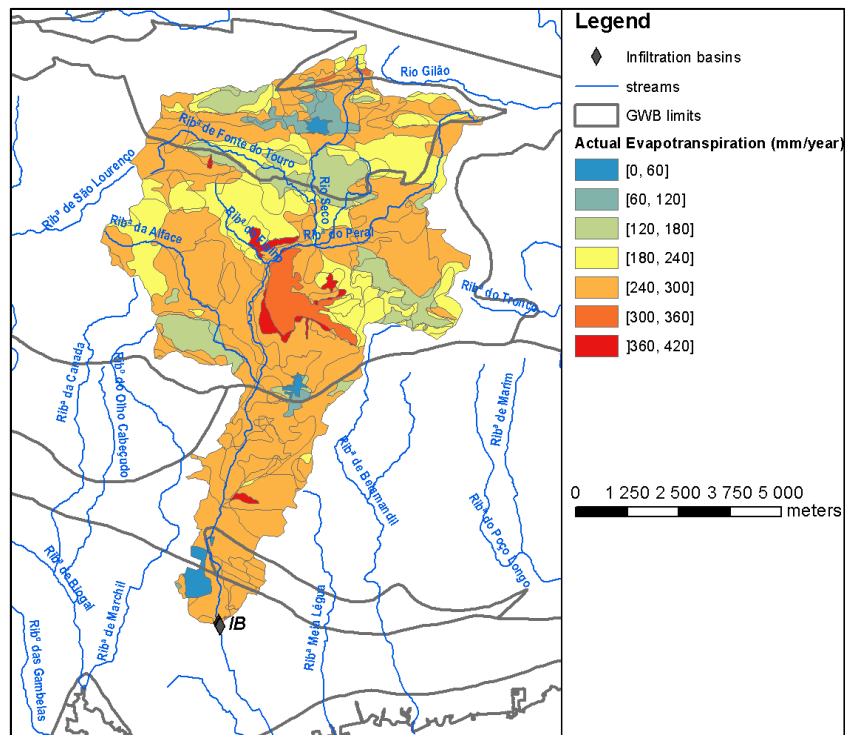


Figure 14 – Average actual evapotranspiration distribution in Rio Seco hydrographic basin upstream the infiltration basins





As a general rule it is expected that precipitation falling inside the hydrographic basin will originate surface runoff to Rio Seco or will infiltrate in the soil, recharge the aquifer systems and eventually discharge in direction to the Rio Seco water course or its tributaries. This means that in a natural dynamic equilibrium surface-ground water system, all the water that recharges the aquifer system, if not used by plants in shallow systems will eventually be part of the surface flow that passes in the MAR facilities. However two different processes may inhibit this equilibrium, first natural groundwater flow may be in a direction outward of the hydrographic basin, and this could be mainly expected in the case of the presence of karstic aquifer systems with regional flow directions different from the surface ones, and secondly anthropogenic abstraction of groundwater may lower the value of the discharge groundwater to the surface medium. It must be stated that the opposite from the first situation may also occur, i.e. water that recharges the aquifer system outside the hydrographic basin and that flows and discharges into the river network of the hydrographic basin (inward flow).

The São Brás de Alportel aquifer system is unconfined to confined, karstic, 34.4 km<sup>2</sup> area, where according with Almeida *et al.* (2000) natural recharge may be concentrated in sinkholes, or diffuse in epikarst structures (*lapias* fields) that occur in some areas; this aquifer system is divided into independent blocks. Almeida *et al.* (2000) refer to an ephemeral resurgence in Rio Seco, which is an indication of groundwater flow discharging into the hydrographic basin. It will be assumed that the groundwater flow divides coincide with the hydrographic basin meaning that all the precipitation water that falls inside the hydrographic basin and infiltrates will not flow outward and that there is no water infiltrating outside the hydrographic basin that will flow inward.

The Chão da Cevada-Quinta de João de Ourém aquifer system is also unconfined to confined, karstic, 5.3 km<sup>2</sup> area (Almeida *et al.*, 2000), where the natural replenishment seems to equilibrate the groundwater abstractions, which is demonstrated by the groundwater level behaviour. Accordingly with Almeida *et al.* (2000) it is not possible to define groundwater flow directions. The western edge of the aquifer system coincides with the Rio Seco river. To the east of the hydrographic basin, other water courses cross this aquifer system, also in a north-south direction. It is assumed that the water that infiltrates in the hydrographic basin will flow to the Rio Seco river.

The São João da Venda-Quelfes aquifer system is multilayer, with two sequences, the lower one mainly detrital and the upper one consisting of marly limestone (Almeida *et al.*, 2000). The system extends over an area of 113 km<sup>2</sup> and its central part is crossed by the Rio Seco hydrographic basin. It is assumed that water that infiltrates in the hydrographic basin will flow to the Rio Seco river.

Finally, the “Orla Meridional Indiferenciado das Bacias das Ribeiras do Sotavento” groundwater body consists of different hydrogeological materials, with no significant hydrogeological importance that would have allowed any of them to be individualised as an aquifer system. This groundwater body extends over an area of 409 km<sup>2</sup>, and is mainly composed of detrital and carbonate materials of Meso-Cenozoic age occurring in the western hydrographic basins of the Algarve. It is assumed that water that infiltrates in the hydrographic basin will flow towards the Rio Seco river.

### Greenhouse rooftops

One future possible important source of water for MAR in the Campina de Faro aquifer system (CFAS) consists in harvested rainwater collected from greenhouse rooftops (Figure 16) due to the large surface area occupied by these infrastructures. This potential source of water could, in some cases, be redirected to large diameter wells (Figure 17), which, at CFAS, present a high potential for

well water recharge, up to 53 m/d, as determined during large well injection tests described in Deliverable 4.3.



**Figure 16 – Intensive greenhouse agricultural activity in the Campina de Faro aquifer system and traditional system of drains for collection of rainwater**



**Figure 17 – Traditional large diameter wells potentially suited for injection of harvested water**

#### **2.1.4 Water origin for MAR (water budget)**

Based on the results of Task 4.1 “Recharge water availability” and according to the values presented on Deliverables 4.1 and 12.1 of MARSOL project, it was estimated an amount of 1.63 hm<sup>3</sup>/year of source water for MAR that could be harvested at the rooftops of the greenhouses.

Rainwater intercepted by greenhouses was estimated taking into consideration the overlapping of distribution of average annual and monthly rainwater with the location of greenhouses at Campina de Faro aquifer system. Average annual rainfall estimates were based on a 32 year average rainfall distribution model (from 1959/60 to 1990/91) consisting in a 1 km<sup>2</sup> resolution matrix developed by Nicolau (2002) and accounts 570 mm/year for Campina de Faro aquifer. The location of greenhouses and their surface area estimation was based on the survey of the land use, using aerial photos from the year 2007, developed by the Algarve Water Basin Regional Administration of the Portuguese Environment Agency (APA-ARH Algarve, unpublished) and sum up a total area of 2.74 km<sup>2</sup> at Campina de Faro aquifer.

In order to estimate the potential rainwater that can be harvested from greenhouses the average distribution of annual and monthly value of rainwater was calculated and overlapped with the location of greenhouses at CFAS.

Figure 18 presents the results for average annual rainfall estimates based on a 32 year average rainfall distribution model (from 1959/60 to 1990/91) consisting in a 1 km<sup>2</sup> resolution matrix developed by Nicolau (2002). Based on this distribution model, average annual rainfall on the CFAS was estimated as 570 mm with the spatial distribution.

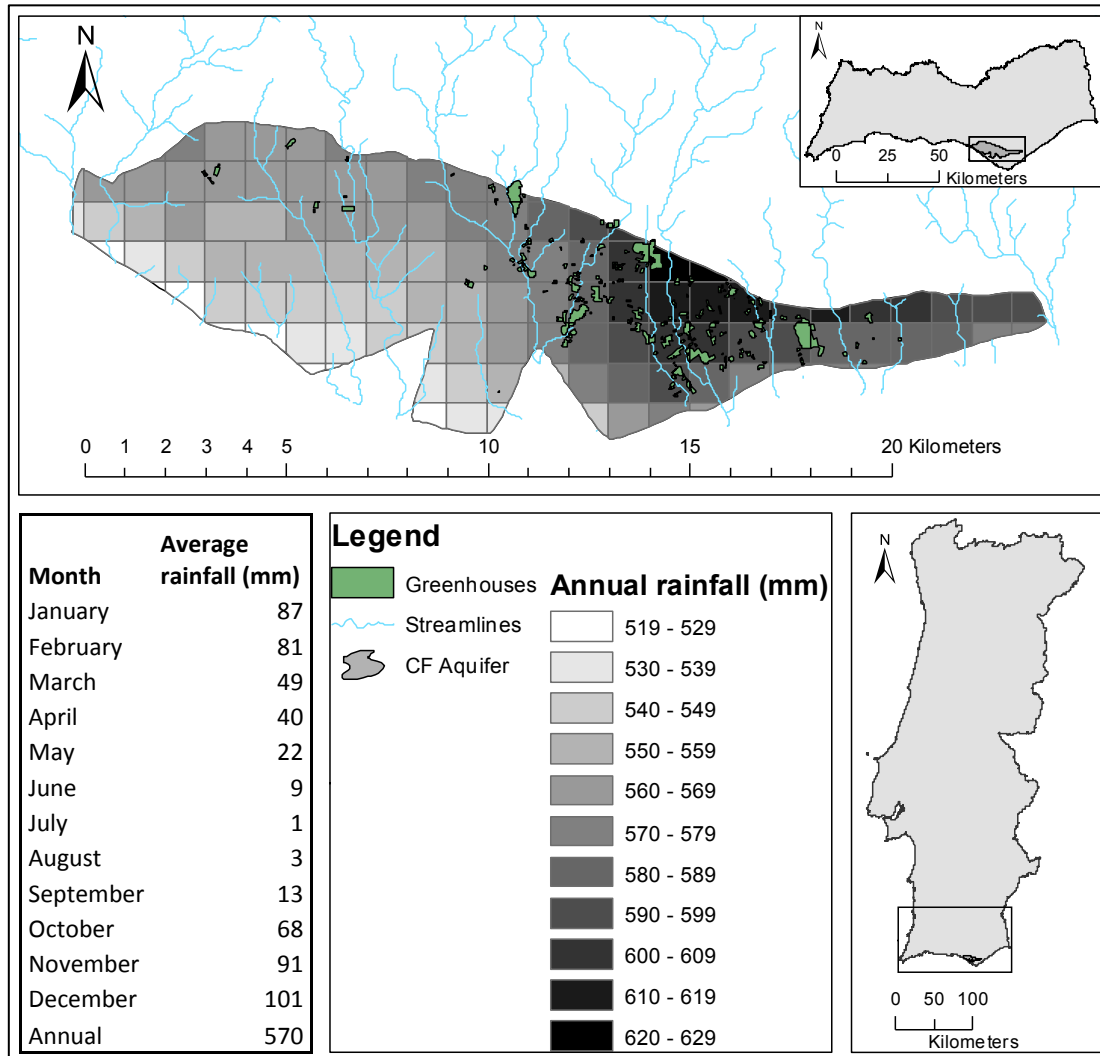


**Figure 18 – Top: 32 year average annual rainfall spatial distribution on Campina de Faro aquifer system (CFAS) (based on Nicolau, 2002) and greenhouse’s locations (based on APA-ARH Algarve, unpublished). Bottom left: 32 year average monthly and annual rainfall distribution values for the CFAS (based on Nicolau, 2002)**

The 32 year monthly and annual averages of rainfall intercepted by the greenhouses are presented in Table 2. It is unlikely that the totality of these amounts can be harvested and used for MAR due to the lack of appropriate greenhouse infrastructures, conduits or close location to large diameter wells.

Nonetheless they should be seen as the average maximum potential water available for future MAR solutions.

**Table 2 – Estimated average monthly and annual potential rainfall harvested from greenhouses**

Month	Intercepted rainfall (hm <sup>3</sup> )	Month	Intercepted rainfall (hm <sup>3</sup> )
JAN	0.252	JUL	0.00273
FEB	0.235	AUG	0.00823
MAR	0.139	SEP	0.0371
APR	0.112	OCT	0.191
MAY	0.0625	NOV	0.263
JUN	0.0275	DEC	0.292
<b>Annual</b>			<b>1.63</b>

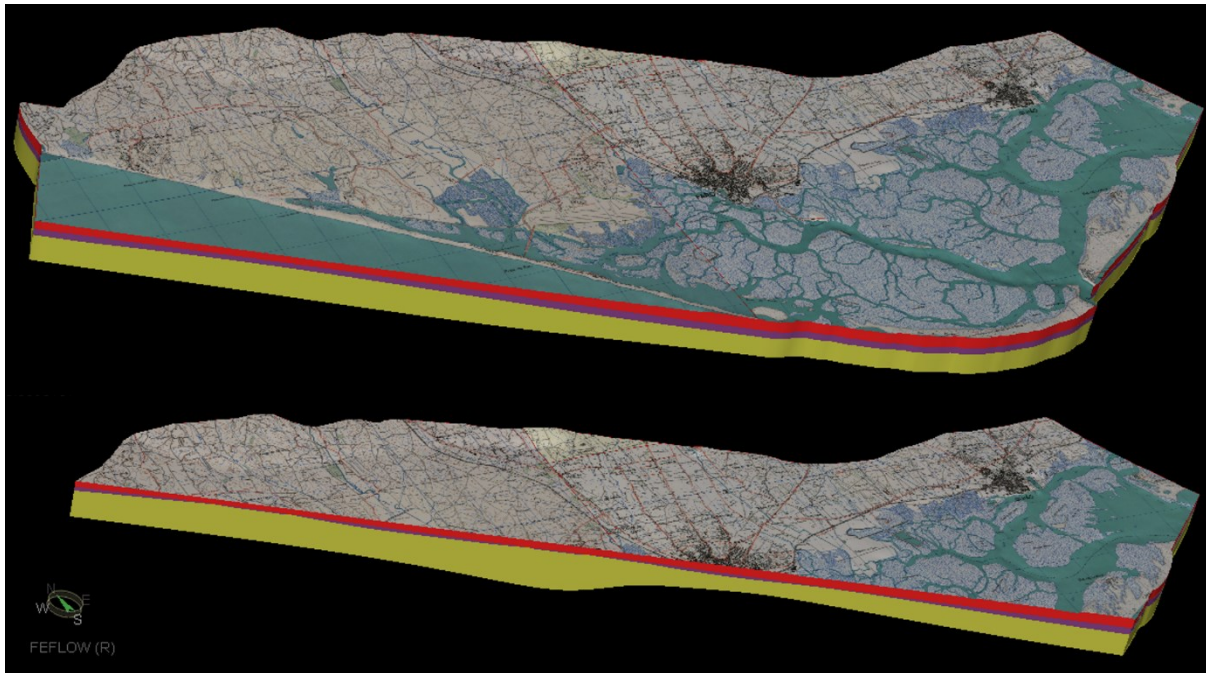
The estimated available water from rainwater collected at greenhouses was estimated at 1.63 hm<sup>3</sup>/yr, and was applied into a transport and flow model of CF aquifer in order to evaluate the effect it could have on the Nitrate contamination in the aquifer.

### 2.1.5 Numerical groundwater flow and transport model for Campina de Faro aquifer

#### 3D model geometry

The Campina de Faro aquifer flow and mass transport model is continuously being developed. The model geometry takes into consideration the 3D structure of the aquifer, which is described in Deliverable 4.2 of MARSOL project. Two aquifer formations and an aquitard are represented in the 3D model geometry. The uppermost aquifer formation is formed by fine sands, sand and gravels from the Miocene and Plio-Quaternary with an average thickness of 50 m. The bottom aquifer consists of a confined aquifer composed by Miocene fossil-rich sandy-limestone deposits, with an irregular thickness that can reach up to 200 m. A confining layer is located between the two aquifers, which is composed by several silty-clayey-sandy layers with variable thickness (Figure 19).





*Note: the top sandy Miocene formation (Red), the bottom marly limestone Miocene formation (yellow) and the intermediate aquitard (purple). The top image shows the complete aquifer plus the sea extension which has also been included in the model. The bottom image presents a cross section of the model showing the layer thickness variation*

**Figure 19 – Vertical structure of the 3D Campina de Faro aquifer model**

In total, the model is composed of 18 layers, the layers 1 – 6 represent the top sandy Miocene aquifer formation, layers 7 – 9 correspond to the confining layer and layers 10 – 18 represent the bottom marly limestone Miocene aquifer formation. In total, the model comprises 480 024 elements and 258 799 nodes.

### **Numerical model parameters, calibration and boundary conditions**

Regarding fluid flow, Dirichlet boundary conditions were set on the first slice of the coastal lagoon corresponding area, with value equal to the mean sea level. Fluid-flux Neumann boundary conditions were applied to the influent stretches of the streams crossing the aquifer (slices 1 and 2), to account for the observed inflow from the streams. Fluid-Transfer Cauchy boundary conditions were applied to the location of a geologic fault feeding the lower slices of the aquifer (slices 18 and 19) from northernmost formations. Well boundary conditions were applied on known location of wells. Abstraction values per well were estimated according to the corresponding irrigated area in which the well is located.

Concerning mass transport boundary conditions, Neumann mass-flux boundary conditions were applied to agricultural areas, with a constant in-flow rate of  $0.03836 \text{ g/m}^2/\text{d}$  solely on the first slice of the model. Dirichlet constant mass-concentration boundary conditions were applied to all in-flow boundaries (streams, lateral flow) with value equal to  $0 \text{ mg/l}$  to represent possible inflow from these sources. Additionally, Dirichlet constant mass-concentration boundary conditions coupled to

minimum mass-flux constrain were applied to out-flow boundary conditions (sea, Ria Formosa coastal lagoon), in order to guarantee exclusively out-flux at these locations.

Model parameters were calibrated regarding flow parameters with FePEST and mass-transport parameters by trial and error in order and results were validated with nitrate observed values from 1995 until 2014 (Figure 4).

Observed simulated spatial distribution of nitrate concentration is similar to observed, though some anomalies were identified. It is likely that these anomalies are not related with agriculture distribution in the model, but may be associated to hydrogeological barriers to flow.

## Results

After running the model for 30 years with the referred nitrate intake, it was observed that nitrate concentration was still slightly underestimated. This could be due to either unaccounted sources of nitrates or, most likely, to the lack of a fresh-saltwater interface in the model, which would hold back some of the nitrates in the model. Figure 20 shows the observed and simulated nitrate concentration.

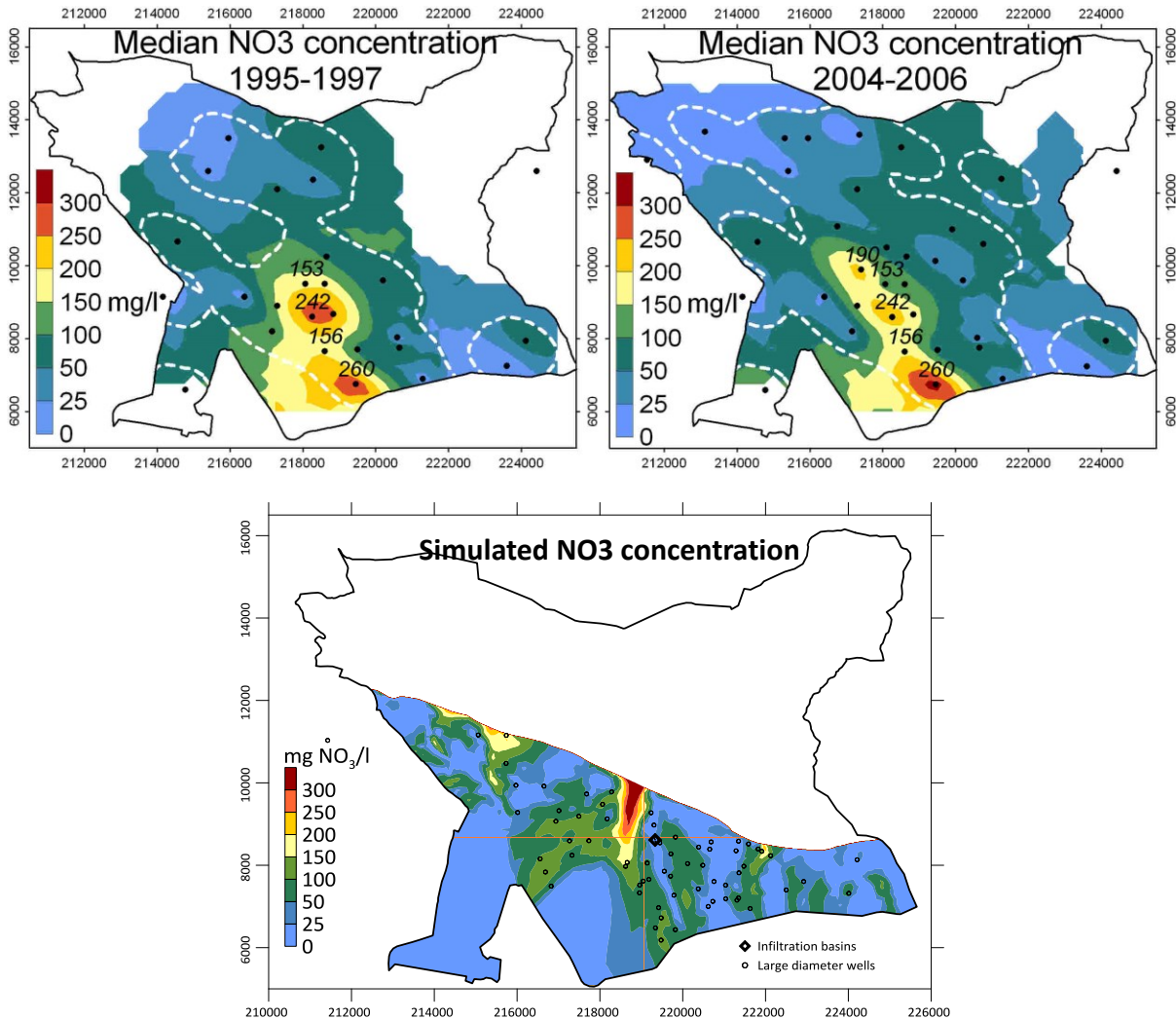


**Figure 20 – Observed (top) nitrate concentration and simulated nitrated contamination after calibration of flow and mass-transport model parameters**

Figure 21 and Figure 22 show some of the results achieved with this simulations for 30 years. From these, it can be seen that the implementation of MAR from the greenhouses, which would be equivalent to  $1.63 \text{ hm}^3/\text{yr}$  would slightly improve the quality of the water. In particular, the nitrate concentration of the lower layers of the upper aquifer would decrease to values below  $50 \text{ mg/L}$ . In the upper layers of the upper aquifer, a reduction of nitrates from  $300\text{-}400 \text{ mg/L}$  to around  $200 \text{ mg/L}$  is observed. This scenario does not consider changes in the fertilization practices.

Regarding the lower Miocene aquifer, it can be seen that the implementation of MAR would contribute to reduce the size of the contamination plume affecting this formation.

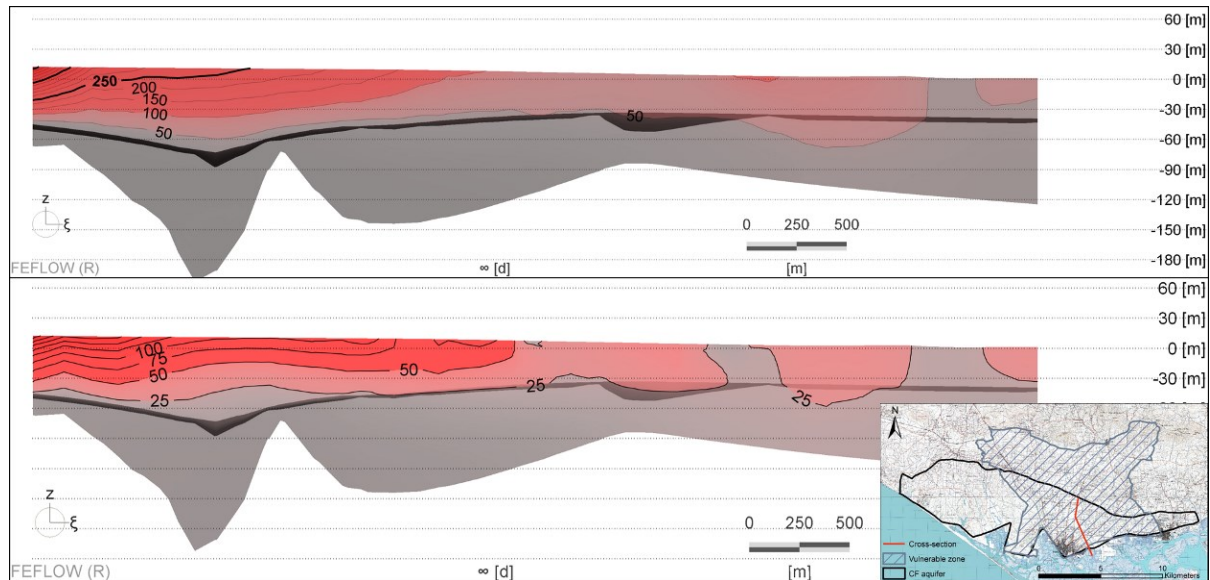


**Figure 21 – Cross-section view of the CF showing nitrate concentration without (top) and with (bottom) the injection of 1.63 hm<sup>3</sup>/year in large wells**

Steady-state  
Current conditions

Steady-state  
MAR of greenhouse runoff in large diameter wells

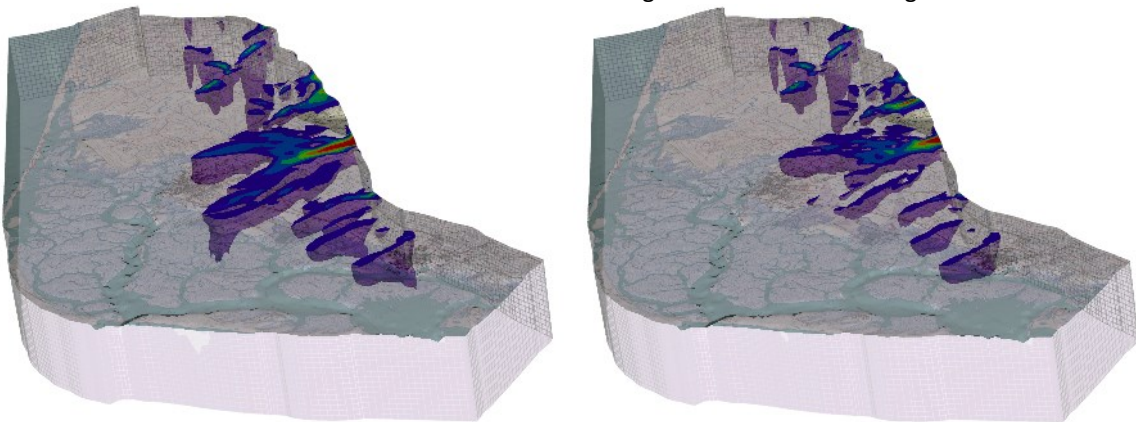


**Figure 22 – 3D view of the nitrate contamination plume at CF without (left) and with (right) the injection of 1.63 hm<sup>3</sup>/year in large wells**



## 2.2 PT2: QUERENÇA-SILVES LIMESTONE KARSTIC AQUIFER SYSTEM (ALGARVE)

### 2.2.1 Introduction and objective

#### Conceptual model

The conceptual model of Querença-Silves aquifer system is detailed on Deliverable 4.2 from where this synthesis text was withdrawn.

The Querença-Silves aquifer system (Figure 23) is the largest aquifer in Algarve, located in the center of the Algarve region, in south Portugal, a region characterized by a Mediterranean climate with dry and warm summers and cool wet winters. It is considered a karst aquifer formed by Jurassic (Lias-Dogger) carbonate sedimentary rocks covering an irregular area of 324 km<sup>2</sup> from the Arade River (at the west) to the village of Querença (at the East) (Monteiro *et al.*, 2006 and Monteiro *et al.*, 2007). The system is delimited south by the Algibre thrust, which is the main onshore thrust in the Algarve Basin, separating the Lower/Early and the Upper/Late Jurassic and to the north by the Triassic-Hettangian rocks (Terrinha, 1998). The Estômbar springs on the west limit of QS aquifer constitute the main discharge area of the system towards the Arade River, supporting several important groundwater dependent ecosystems.

Manuppella *et al.*, (1993) presents a cross-section of the central Algarve region (Figure 24). This cross-section allows a synthesized visualization of the geometric relations of the Early/Lower Jurassic lithology which support the Querença-Silves aquifer system Identified in blue, in Figure 24.

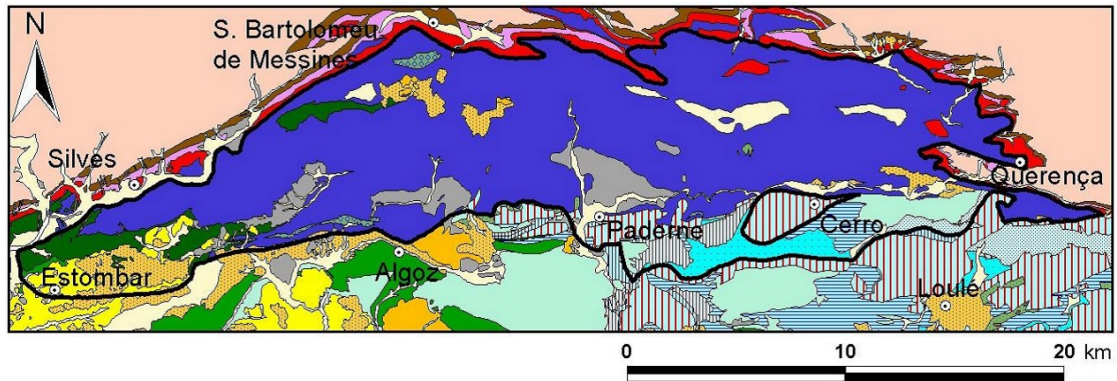


Figure 23 – Querença-Silves aquifer system’s geology. Underlined features are the ones identified within the aquifer limits. Almeida *et al.* (2000)

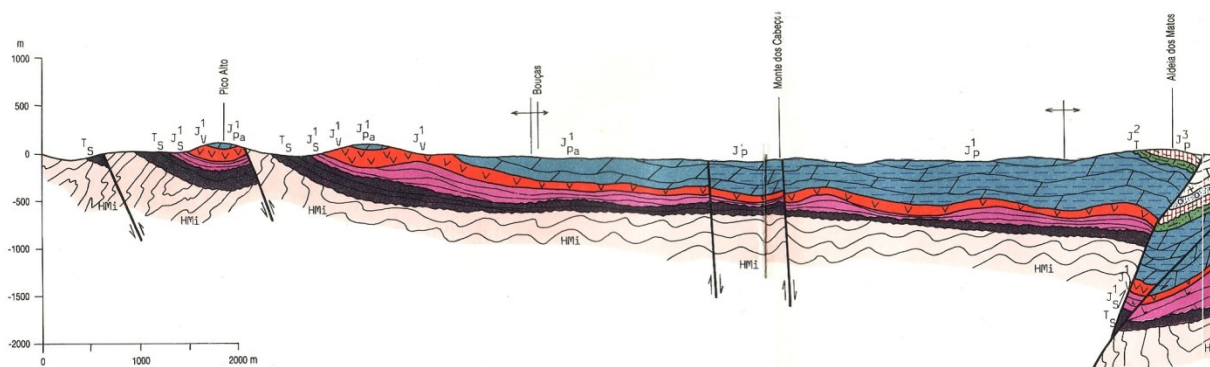
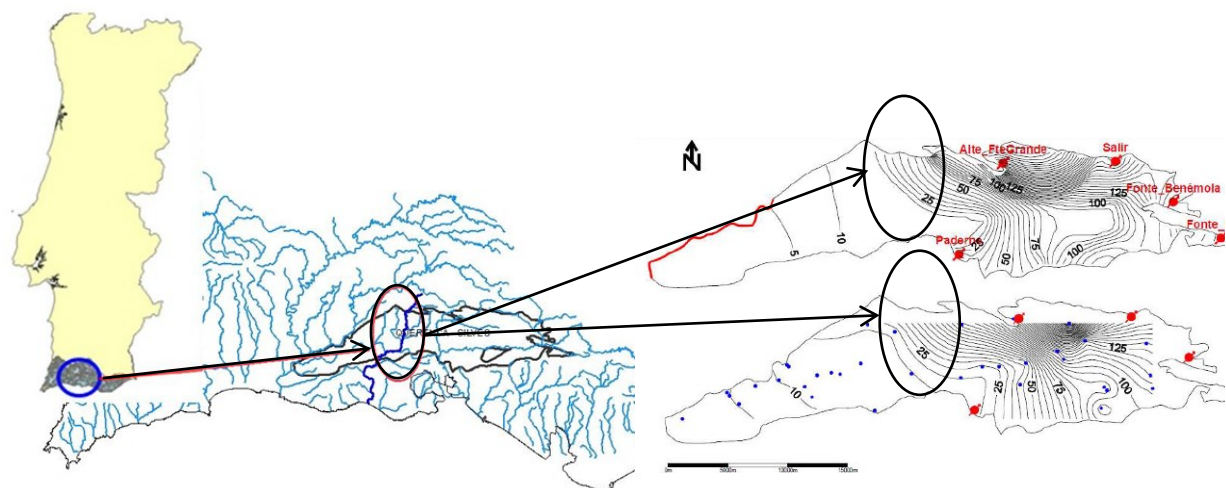


Figure 24 – Geometry of the carbonated rocks of early Jurassic which constitute the most important support of the aquifer system Querença-Silves (dark blue colour, to the left of the Algre thrust). Adapted from Manuppella *et al.* (1993)

Accordingly to previous studies, the hydrogeological setting of the Querença-Silves karstic aquifer, has a complex compartmented structure, with two distinct domains separated by a fault: a western

domain and an eastern domain. Its western domain has a well-developed karst, westward flow direction, with the main discharge areas along the Arade river, with particular relevance to Estômbar springs (westernmost point). Its eastern domain has more random flow directions, less regular piezometric surfaces (Figure 25) and a lower karst development. The tectonic activity of this region results in its widespread fracturing, defining a significant number of semi-independent aquifer blocks, with more or less constrained and restricted hydraulic links between them. Such hydraulic restrictions are more expressive in the eastern domain, because in the western domain the pervasive karstic network largely obliterates such tectonic setting (Mendonça and Almeida, 2003; Monteiro *et al.*, 2006).



Monteiro *et al.*, 2006

**Figure 25 – Site location along Ribeiro Meirinho stream and central-western area of Querença-Silves aquifer and its piezometry (upper right: modelled; lower right: measured) (Leitão *et al.*, 2014)**

The Ribeiro Meirinho stream is located in the central-western area of Querença-Silves aquifer and its upper reaches are located outside the aquifer, in Serra Algarvia. The latter are Palaeozoic terrains, composed mainly of schist and graywakes, essentially impervious lithologies, being therefore, the main source of water for this stream until it reaches the Jurassic limestones, dolomites, dolomitic limestones and other, less important, calcareous formations composing the karst aquifer of Querença-Silves.

### **Geophysical surveys, with the resistivity method, for PT Querença-Silves demo site conceptual model**

#### Methodology

Two geophysical surveys, with the resistivity method, were performed in PT Querença-Silves Demo site (Cerro do Bardo) with the main objective of assessing the groundwater flow direction in the test site (Figure 26). To achieve this purpose two water recharge tests were performed: the first one in 2014 and the second one in 2016.

The first survey took place during one week with injection of water mixed with salt (in the second day) in a well. A time-lapse resistivity survey was performed on three alignments crossing each other near the well. Salt was selected as a tracer due to its capability to reduce water resistivity and to

enhance the possibility of identifying the water circulation with the geophysical electrical resistivity method. Data was collected more than once in each alignment/profile, during that week, in a total of 15 profiles gathered (cf. Table 3).



**Figure 26 – Geophysical field work in 2014. Processing data on site**

The second survey took place in 2016 along two alignments selected based on the knowledge already gathered for the site and it was completed in three phases: a reference position for each of the alignments, prior to the salt (1 ton) and water injection in the well; three days monitoring during the water injection period; and two days of monitoring starting two days after the end of water injection.

Profile P1 monitoring was performed using the dipole-dipole array, and Wenner array was the method selected for profile P2. This combination was chosen after analysing 5 reference profiles gathered with both arrays on P1 and P2 during the first phase, in order to allow a maximization of data collected with the available equipment without having to move it from one alignment to the other as happened in 2014's survey. With this strategy a total of 42 profiles were collected during the monitoring period with the rejection of one of them, on P2, due to wrong connections when resuming the third phase (cf. Table 4).

**Table 3 – Summary of the 2014' geophysical survey**

Conditions	Date	Profile 1			Profile 2			Profile 3		
		Time (1)	Time (2)	Time (3)	Time (1)	Time (2)	Time (3)	Time (1)	Time (2)	Time (3)
Reference		December 15, 2014			December 16, 2016 - 11:15/12:15			December 16, 2014		
Water injection (4)	December 16, 2014	13:15	+2h50m	---	---	---	---	---	---	---
		---	---	---	---	---	---	15:55	+5h30m	+1h40m
No water	December 17, 2014	11:15	+24h50m	+21h00m	9:40	+23h15m	+19h35m	14:40	+28h15m	+24h25m
	December 18, 2014	10:55	+48h30m	+44h40m	9:20	+46h55m	+43h05m	12:40	+50h15m	+46h25m
		---	---	---	---	---	---	15:30	+53h05m	+49h15m
	December 19, 2014	10:45	+72h20m	+68h30m	9:15	+70h50m	+67h00m	12:25	+74h00m	+70h10m

Notes:

- (1) - Survey begin time
- (2) - Time passed after begin of water injection
- (3) - Time passed after stop of water injection
- (4) - Water injection: begin at 10:25 and stopped at 14:13 on December 16th





**Figure 27 - Geophysical field work in 2016. Portuguese MARSOL team**

**Table 4 – Summary of the 2016’ geophysical survey**

Conditions	Date	Profile 1			Profile 2			
		Time (1)	Time (2)	Time (3)	Time (1)	Time (2)	Time (3)	
Reference		April 14, 2016			April 15, 2016			
After salt		12:00	---	---	---	---	---	
Water injection (4)	April 20, 2016	14:10	+0h10m	---	15:10	+1h10m	---	
		17:10	+3h10m	---	16:48	+2h48m	---	
		18:20	+4h20m	---	17:57	+3h57m	---	
	April 21, 2016	09:30	+19h30m	---	9:10	+19h10m	---	
		11:05	+21h05m	---	10:35	+20h35m	---	
		14:10	+24h10m	---	11:55	+21h55m	---	
		15:30	+25h30m	---	15:00	+25h00m	---	
	April 22, 2016	17:00	+27h00m	---	16:15	+26h15m	---	
		09:45	+43h45m	---	9:15	+43h15m	---	
		11:00	+45h00m	---	10:35	+44h35m	---	
		12:15	+46h15m	---	11:50	+45h50m	---	
		14:15	+48h15m	---	13:52	+47h52m	---	
	No water	April 26, 2016	15:30	+49h30m	---	15:05	+49h05m	---
			16:30	+50h30m	---	16:10	+50h10m	---
			13:05	+143h05m	+53h05m	---	---	---
			14:30	+144h30m	+54h30m	15:20	+145h20m	+55h20m
15:50		+145h50m	+55h50m	16:35	+146h35m	+56h35m		
17:00		+147h00m	+57h00m	17:45	+147h45m	+57h45m		
18:15		+148h15m	+58h15m	---	---	---		
April 27, 2016	09:50	+163h50m	+73h50m	9:30	+163h30m	+73h30m		
	11:05	+165h05m	+75h05m	10:35	+164h35m	+74h35m		

Notes:

- (1) - Survey begin time
- (2) - Time passed after begin of water injection
- (3) - Time passed after stop of water injection
- (4) - Water injection: begin on 4/20 at 14:00, and stop on 4/24 at 8:00

2014’ geophysical survey

Figure 28 presents the location of 2014’ geophysical survey.

Figure 29 to Figure 31 illustrate, for each alignment, the reference resistivity model and the percentage change in resistivity model between a resistivity model and the reference one.

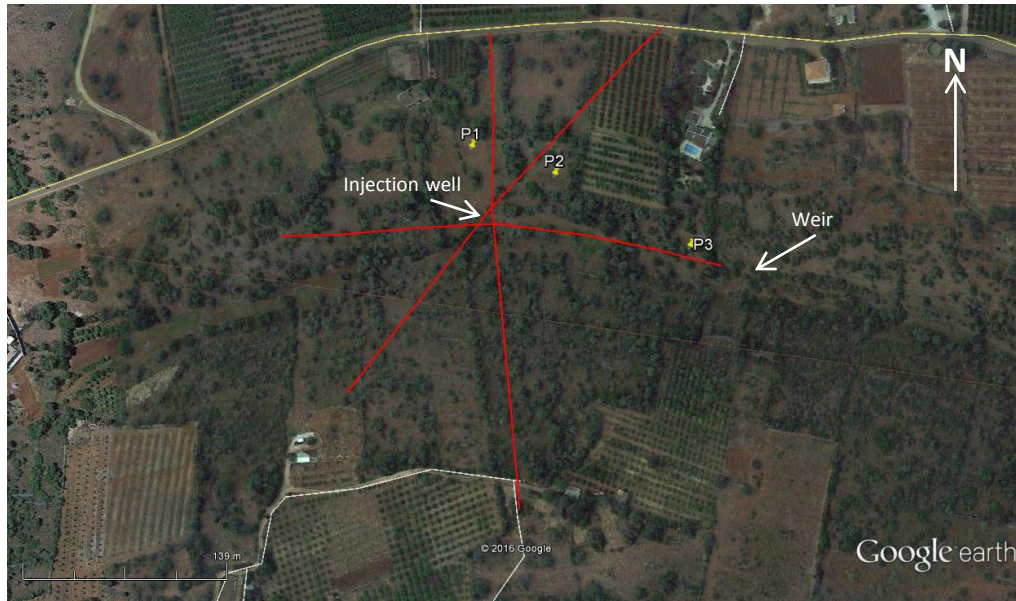


Figure 28 - Location of 2014 geophysical profiles in Querença-Silves aquifer at Cerro do Bardo site

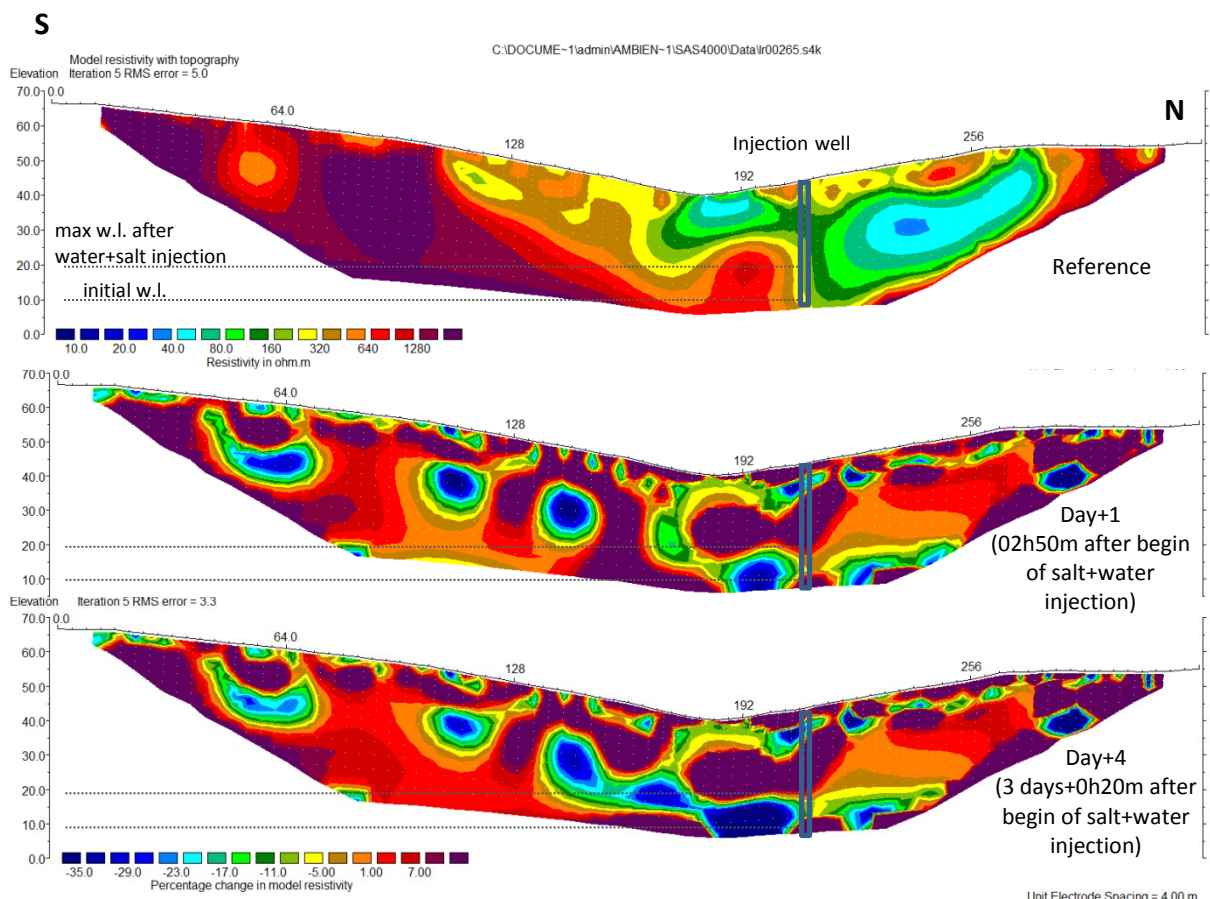
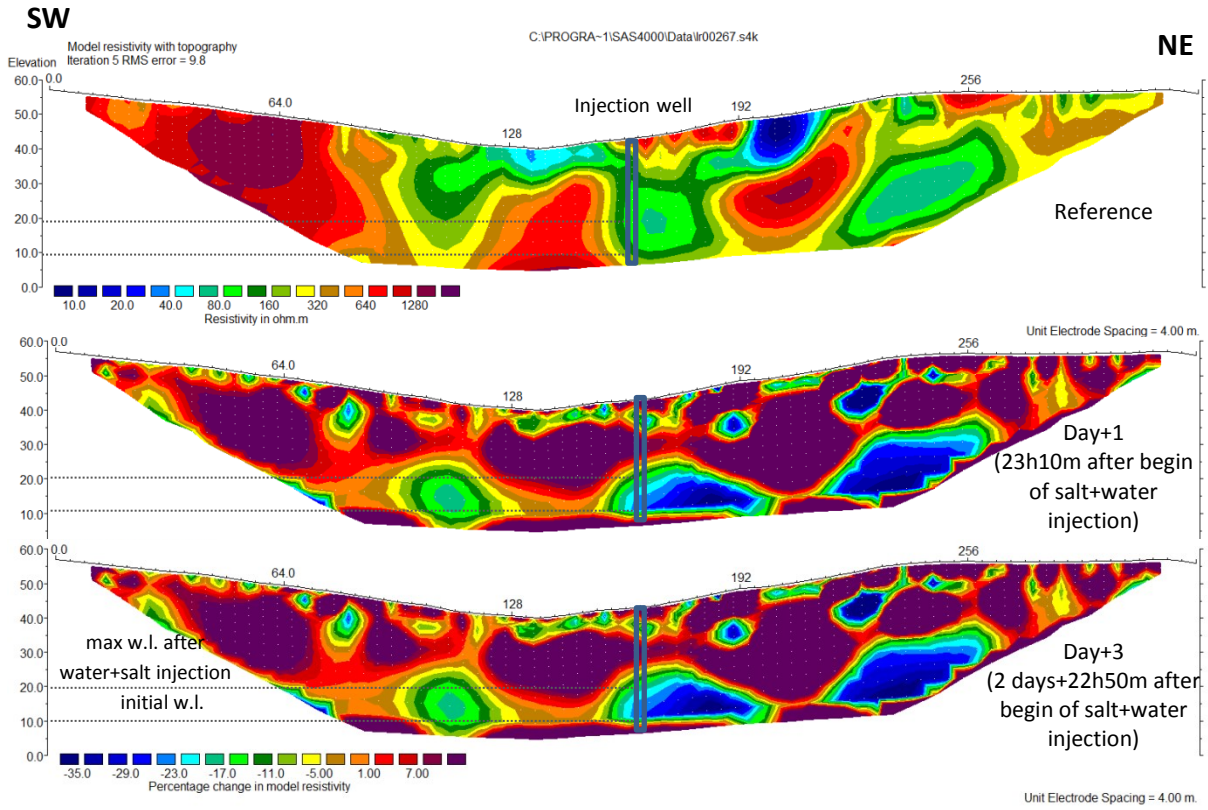
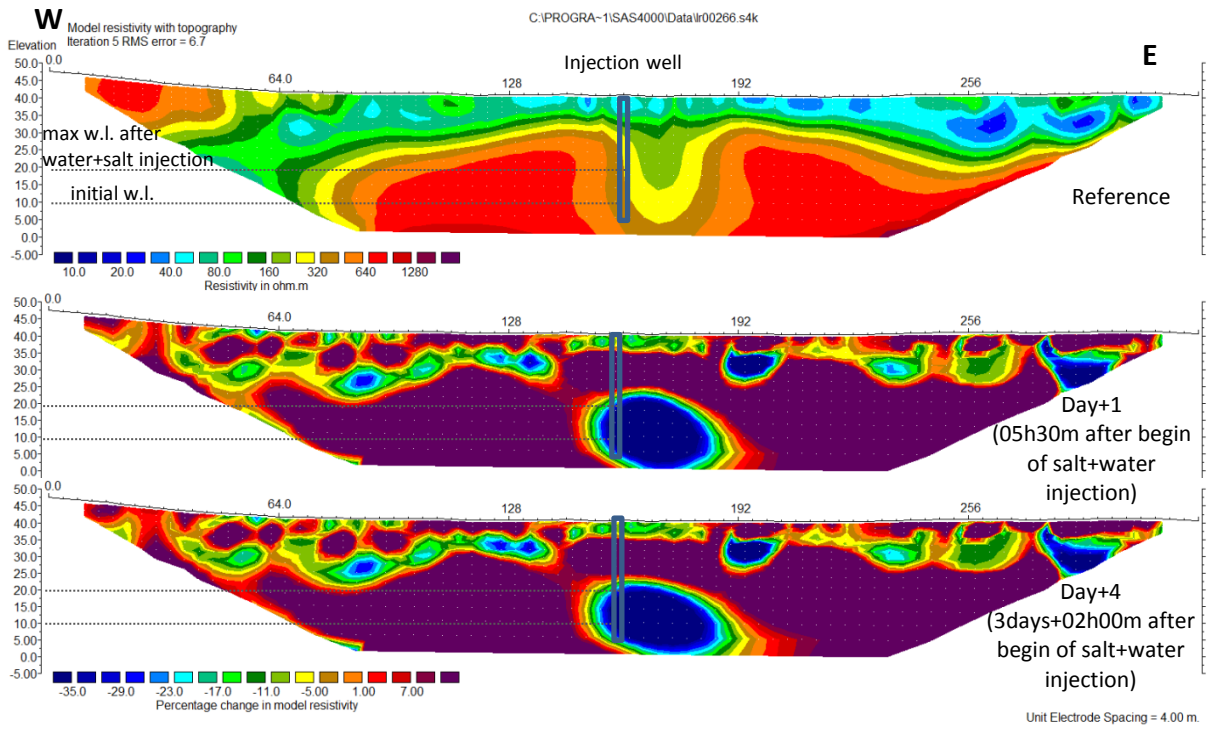


Figure 29 - Geophysical surveys (absolute (reference) and % change) in Querença-Silves aquifer at Cerro do Bardo performed during the injection tracer test of 2014 - results from profile P1





**Figure 30 - Geophysical surveys (absolute (reference) and % change) in Querença-Silves aquifer at Cerro do Bardo performed during the injection tracer test of 2014 - results from profile P2**



**Figure 31 - Geophysical surveys (absolute (reference) and % change) in Querença-Silves aquifer at Cerro do Bardo performed during the injection tracer test of 2014 - results from profile P3**

A first survey (background or reference situation) was performed in the first day in alignment P1, and on the second day in alignments P2 and P3, with P2 readings starting just before the beginning of water injection. The reference in alignment P2 could have been influenced by the injected water (cf. Figure 30).

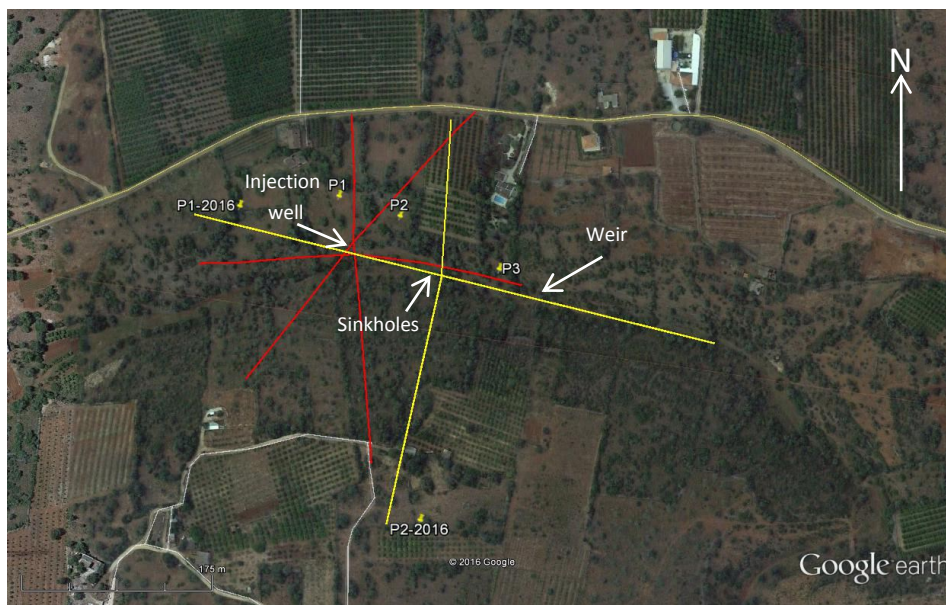
Tomographic images of the subsoil in terms of electrical resistivity and resistivity variation with time were obtained with Res2Dinv v3.56 software.

The survey was performed using the dipole-dipole array with a dipole distance of 8 m, for a total length of 320 m and a research depth of about 30 m for each alignment. After the end of water injection all profiles were repeated in the 4 subsequent days. The objective was to have more information regarding the water pathways in the area with the time-lapse evolution of the resistivity.

From the observation of Figure 29 to Figure 31 one can say that water (blue zone on percentage change in resistivity) flows in the southeaster direction, and at the level of the well bottom.

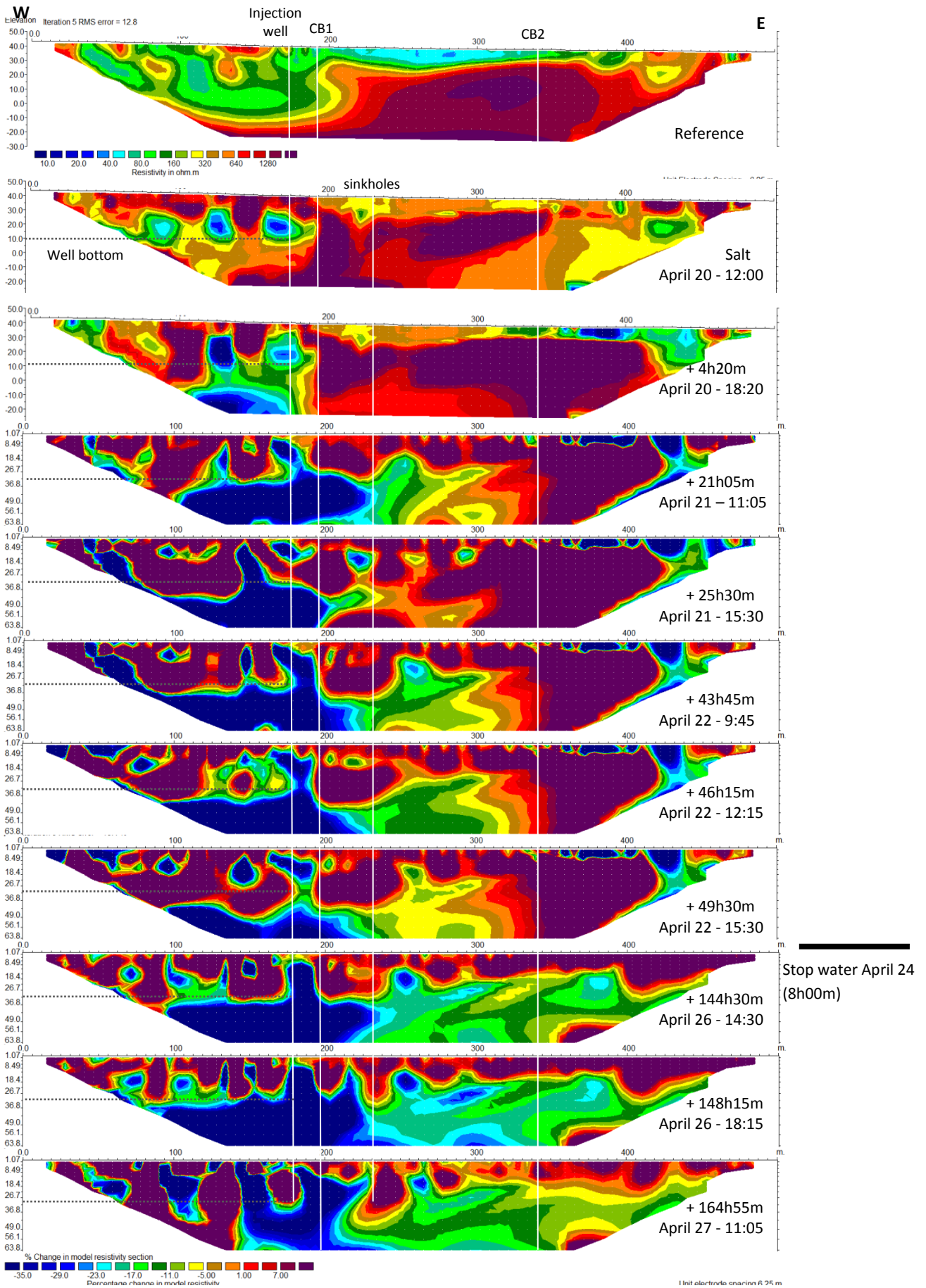
### 2016' geophysical survey

Figure 32 presents the location of both 2014' and 2016' geophysical surveys. Figure 33 and Figure 34 illustrate, for each alignment, the reference resistivity model and the percentage change in resistivity model between some resistivity model and the corresponding reference one (white lines depicts the position of reference infrastructures). 2016' survey was performed with a dipole distance of 12.5 m which leads to a length of 500 m for P1 and 250 m for P2, since the latter was executed with half of the cables. The maximum investigation depth reached about 64 m on profile P1. Profile P2 was installed very close to the sinkholes and reached about 40 m in depth.



**Figure 32 – Location of 2014 and 2016 geophysical profiles in Querença-Silves aquifer at Cerro do Bardo site**





**Figure 33 - Geophysical surveys (absolute (reference) and % change) in Querença-Silves aquifer at Cerro do Bardo performed during the large injection tracer test of 2016 - results from profile P1**

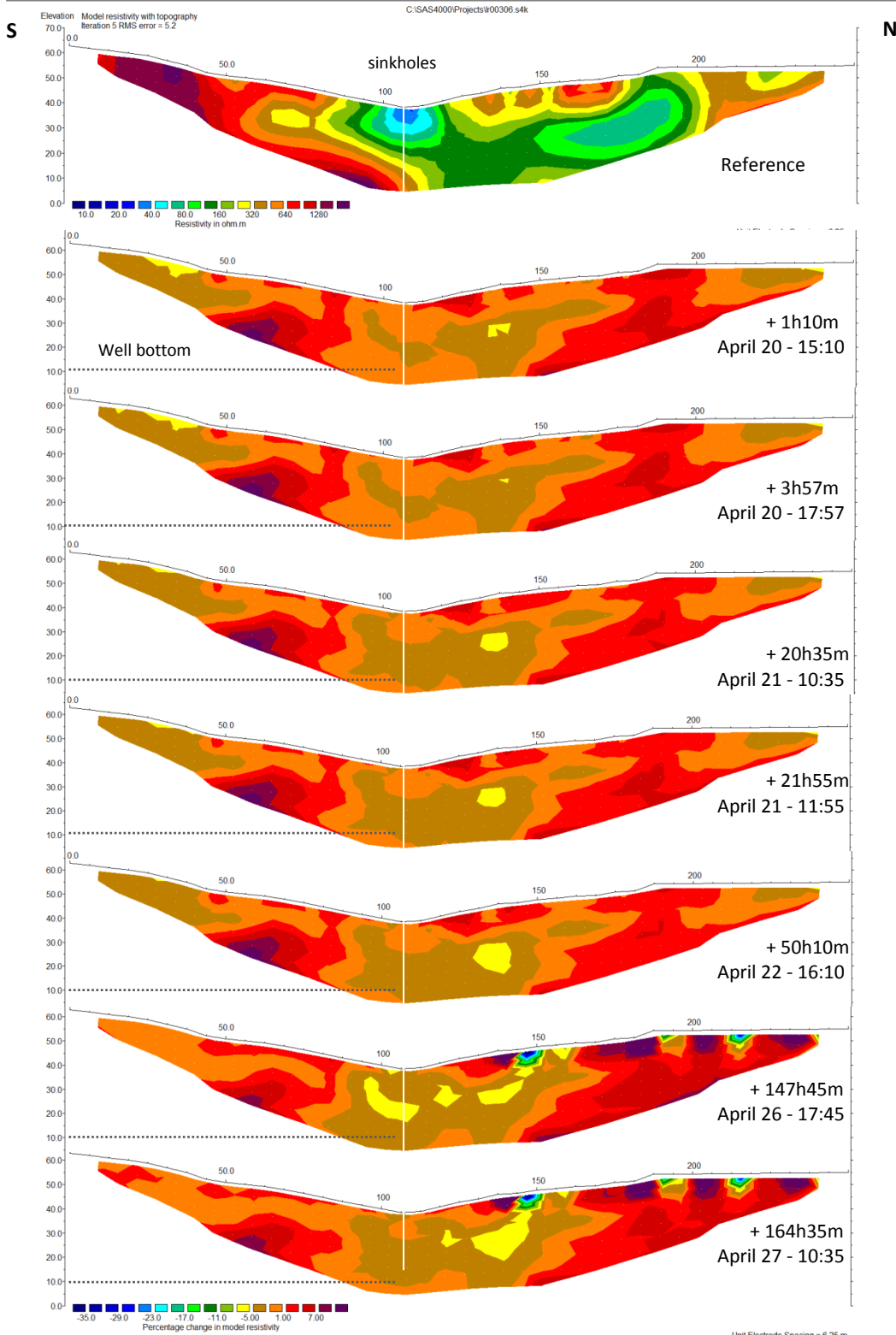


**Figure 34 - Geophysical surveys (absolute (reference) and % change) in Querença-Silves aquifer at Cerro do Bardo performed during the large injection tracer test of 2016 - results from profile P2**

From the observation of Figure 33 and Figure 34, namely the sections of percentage change in resistivity model, one can conclude that water flows mainly towards the west direction and downwards, although there is also some flow in the east-southeaster direction as it was seen from the 2014' results. During the test, after 3 hours of injection, about 1/3 of the injected water started flowing into the sinkholes. All this amount of water and that flowing underground is revealed from

the sections as a change of about 15-20% (at the top – P2 – 10% at the maximum) which compares with a change higher than 30% westward and downwards from the well. The conjunction of this feature with the fact that the resistivity of the eastern zone is much higher than that near the well, may indicate that this zone of the massif has higher porosity probably revealing a more developed karst.

### Modelling context

A 3D finite element flow and transport, calibrated and validated, model is being used to study and predict the regional effect of injecting wet year's surface water surplus in the large diameter Cerro do Bardo well and surrounding area.

This analysis was performed under steady-state conditions and considered two water supply abstractions scenarios. Scenario 1 which is equivalent to the current extraction conditions and scenario 2 which is equivalent to the maximum abstraction period ever registered at QS aquifer, which corresponds to the drought of 2004/2005.

The Querença-Silves aquifer system supported an important part of the Algarve urban water supply system during the severe drought that affected Portugal during 2004 and 2005. During this period the extractions in the QS were the most intense in all the historic period of water use in the Algarve region. The extraction volumes for urban supply in municipalities settled in the area of the QS in this period were:  $4.6 \times 10^6$  m<sup>3</sup>/year (Silves);  $1.9 \times 10^6$  m<sup>3</sup>/year (Lagoa);  $3.5 \times 10^6$  m<sup>3</sup>/year (Albufeira) and  $0.4 \times 10^6$  m<sup>3</sup>/year (Loulé) (Monteiro *et al.*, 2007a). Additionally to these abstractions, Águas do Algarve SA extracted in this same period  $11.0 \times 10^6$  m<sup>3</sup>/year in the Vale da Vila well field (also for urban supply in other areas of the Algarve). Finally, as the average of extractions for irrigation in the area of the QS is in the order of  $30.91 \times 10^6$  m<sup>3</sup>/year (Nunes *et al.*, 2006), it is estimated that the total extractions in the QS, in its period of more intense water exploitation, was in the order of  $52.31 \times 10^6$  m<sup>3</sup>/year. Such extraction scenarios may induce a decrease in the hydraulic head at a regional level in the aquifer and contribute to the intrusion of saltwater coming from the Arade river, at the westernmost border of the aquifer. The location of the main well fields, used for urban supply in QS, is represented in Figure 35.

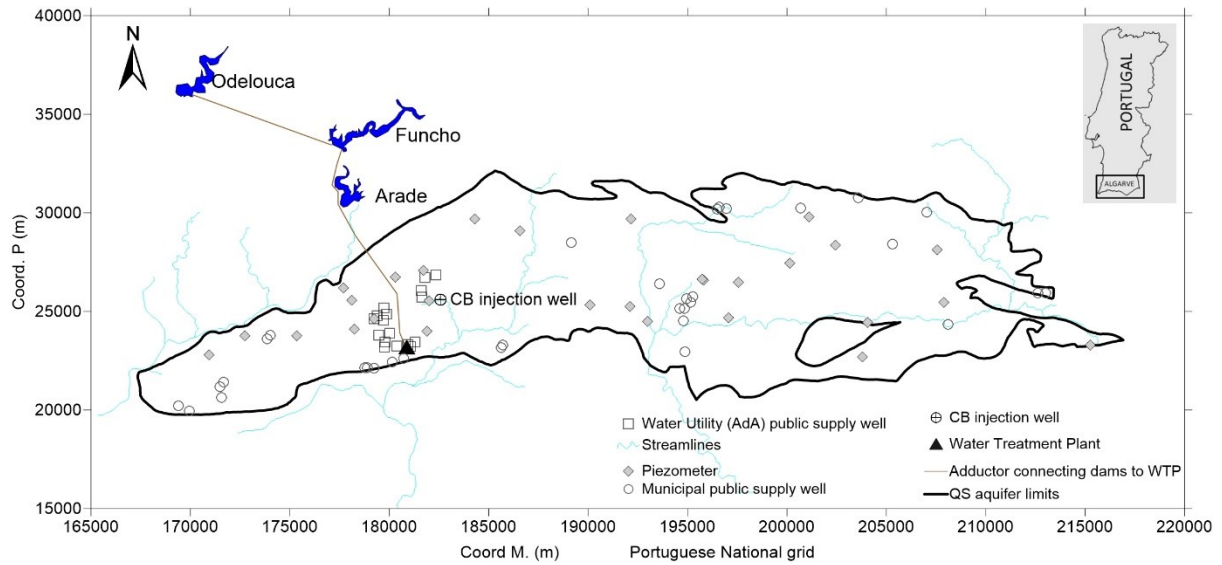


**Figure 35 – Location and main supply wells in Querença-Silves aquifer system**

## 2.2.2 Water balances

### Natural recharge

Oliveira *et al.* (2008) estimated an aquifer balance of  $104 \text{ hm}^3/\text{y}$  with a sequential Daily water balance model, later updated by Oliveira *et al.* (2011) to  $94 \text{ hm}^3/\text{y}$ . This model, BALSEQ\_MOD, estimates a spatial distribution of infiltration by incorporating methodologies to estimate the processes of soil infiltration, real evapotranspiration and deep infiltration. The last estimates from 2011 and its spatial distribution were incorporated into the numerical model, as presented in Figure 36.

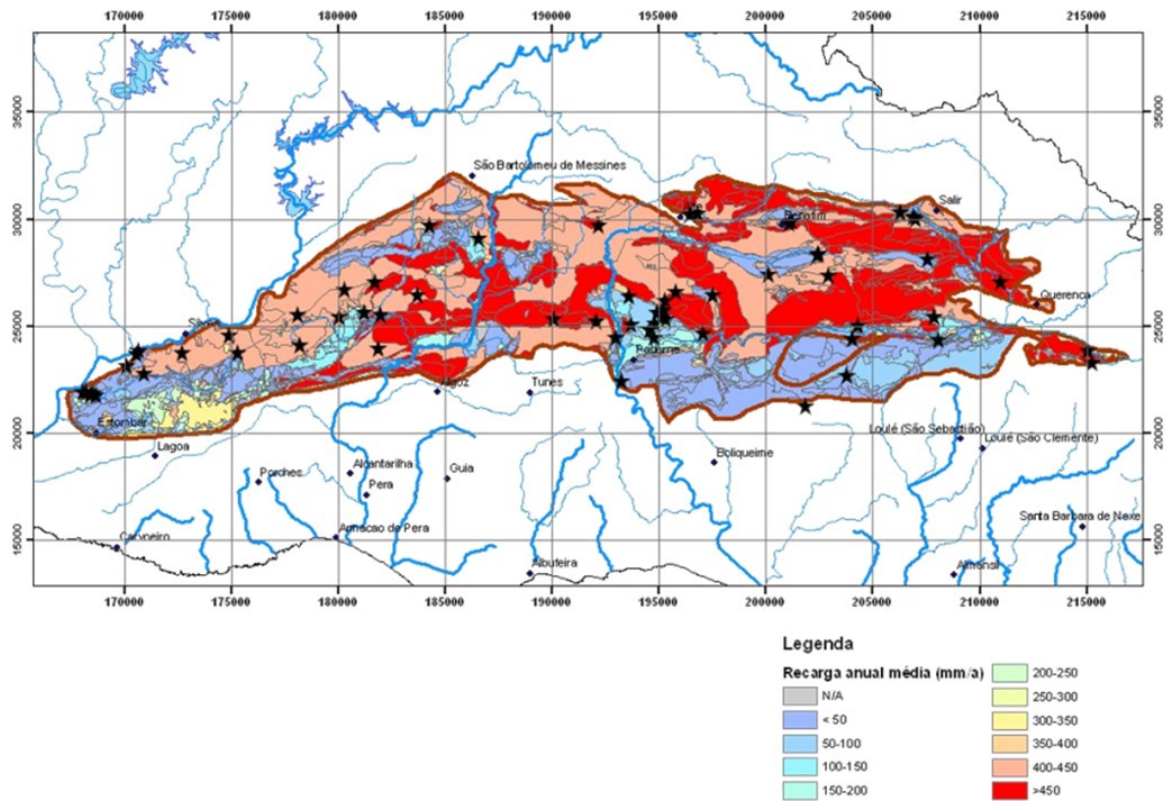


Figure 36 – Average Querença-Silves aquifer recharge (period 1941-1991) (source: Oliveira *et al.* 2008)

### 2.2.3 Infrastructures for MAR

The main infiltration infrastructure at the demo site consists of the CB hand made large well, originally built in the late 1970's, with a diameter of 2 meter and 32 meters deep, located close to Aivados stream at Cerro do Bardo (Figure 35). During MARSOL project, injection tests with and without tracers were performed on the CB well (Deliverable 4.3), the results of which indicated high infiltration capacity (around 400 m/d), with a groundwater flow pattern mostly towards East, contrary to the regional aquifer main flow direction. A weir located 200 m downstream CB well retains eventual water losses from the well when the injected water volume exceeds the injection capacity at the well. These infrastructures provide good conditions for implementing a MAR system, in which the infiltration process is enhanced by natural existing sinkholes in the riverbed. These same sinkholes allow the infiltrated water to reach the regional aquifer.

The areas draining to the location of the three infiltration basins are represented in Figure 15. The river basin of the WWTP of São Bartolomeu de Messines (area = 13.6 km<sup>2</sup>) is included in the river basin of Ribeiro Meirinho (total area = 57.6 km<sup>2</sup>). The river basin of Cerro do Bardo (29.4 km<sup>2</sup>) is west of the previous one. The Cerro do Bardo river basin is almost completely installed on the Querença-Silves aquifer system (unless a small part on the north that belongs to the “Orla Meridional indiferenciado das Bacias das ribeiras do Sotavento” groundwater body (GWB)). The WWTP of São Bartolomeu de Messines river basin is almost exclusively formed by the “Orla Meridional indiferenciado das Bacias das ribeiras do Sotavento” GWB and, in a very small area of 2.0 km<sup>2</sup>, by the



“Zona Sul Portuguesa das Bacias das ribeiras do Sotavento” GWB. Concerning the Ribeiro Meirinho river basin, apart the area included in the WWTP of São Bartolomeu de Messines river basin, is almost exclusively developed on the Querença-Silves aquifer system.

The conceptual model of the Querença-Silves aquifer system is described, as well as a general characterisation of the “Orla Meridional indiferenciado das Bacias das ribeiras do Sotavento” GWB is presented in Deliverable 4.2. Concerning the “Zona Sul Portuguesa das Bacias das ribeiras do Sotavento”, this GWB has a total area of 293 km<sup>2</sup> and is comprised of Paleozoic geological formations that compose the part of the geostuctural unit of the Portuguese South Zone located in the western hydrographic basins of the Algarve. It is a low productivity area mainly composed of schist and greywackes. In this last area it is also assumed that water that infiltrates in the hydrographic basin will flow towards the correspondent water course.

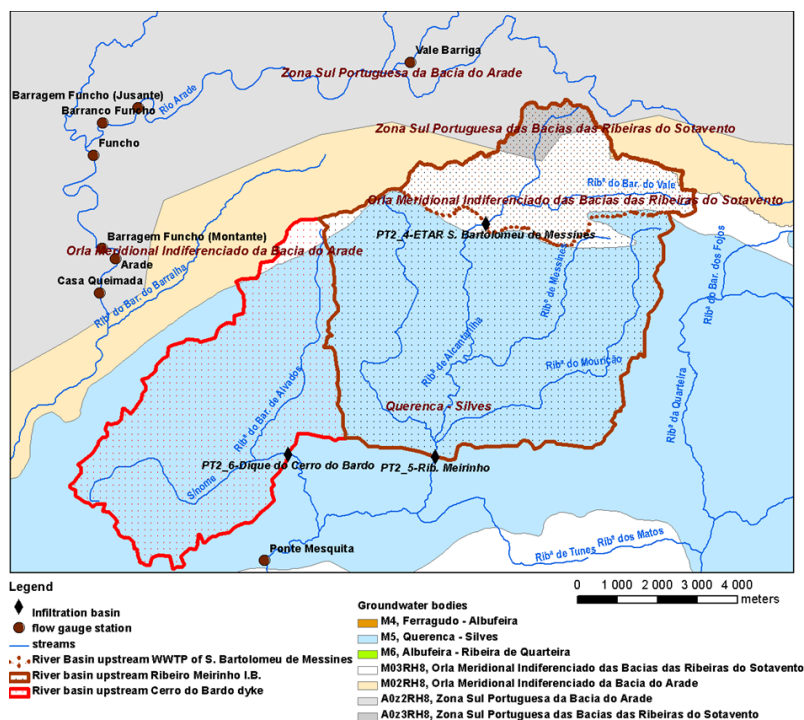


Figure 37 – Hydrographical basin above selected MAR facilities in PT2 and related groundwater bodies

## 2.2.4 Water origin for MAR (water budget)

For the Cerro do Bardo site, the water origin for MAR would be the surplus of surface water dams (Funcho, Odelouca and Bravura), which is typically discharged downstream during wet years. This discharge occurs mostly for security measures when the dams are in risk of reaching full capacity of the reservoir (in order to avoid dam overtopping which would result in serious infrastructure damage), therefore, there is no direct relation between yearly rainfall and the discharged surplus. According to Águas do Algarve, Lda., Odelouca dam alone has an average annual inflow of 122 hm<sup>3</sup>, of which an annual supply to the Alcantarilha WTP is estimated at 50 – 55 hm<sup>3</sup>/year. This would result in an average remainder storage of ~70 hm<sup>3</sup> every year in the Odelouca dam alone.



A part of this surface storage could be used for MAR at the CB well and weir system, which are located upstream the groundwater pumping wells of Alcantarilha WTP. An adductor connecting the three dams to the water treatment plant of Alcantarilha is already active (Figure 35), which passes around 2 km from the Cerro do Bardo well at its closest point. The latter needs to be constructed since all the tests performed - to assess the infiltration capacity of this area - have used a temporary pipeline installed to supply water for the experiment using a well located at a distance of 1.4 km (Deliverable 4.3).

## 2.2.5 Numerical groundwater flow model for Querença-Silves aquifer

### Goals

With the support of numerical models it is intended to show how the Querença-Silves aquifer may be influenced by seasonal pumping effects and how this impacts the regional water level and the evolution of the saltwater-freshwater interface, as well as how MAR can contribute to decrease the level of such impacts and contribute to augment the groundwater piezometric levels. This was done by simulating two extraction scenarios, one scenario with the highest registered abstraction, during the 2004/05 drought and another with the actual abstraction rates. Then, for both scenarios, several MAR variants were tested, injecting from 1 to 25 hm<sup>3</sup>/year at the existing infiltration infrastructures. The results from the large infiltration and tracer test done in April 2016 have shown an infiltration capacity of, at least, 4060 m<sup>3</sup>/d, i.e. 1.48 hm<sup>3</sup>/y (Deliverable 4.3, Leitão *et al.*, 2016).

### Introduction

The model used in this project is the result of ongoing research in relation with monitoring and modelling of aquifers at the University of Algarve. A more detailed review of the evolution and applications and current state of this model can be found in Hugman *et al.* (2012) and Hugman *et al.* (2013).

QS is a karst aquifer, though the developed model flow domain, is represented as a single continuum equivalent porous media. The representation of the flow domain of karst systems as single continuum equivalent porous media, using concepts of hydraulic conductivity (K), is valid when modelling hydraulic heads and flow on a regional scale, as is discussed by Scanlon *et al.* (2003). Notwithstanding, it is important to bear in mind that this methodology may result in significant uncertainty when simulating smaller scale effects such as drawdown of wells at a local scale.

### 3D model geometry

Monteiro *et al.* (2007a) calculated a thickness map of the Querença-Silves aquifer model based on the geological cross section presented by Manuppela (1992) and the maximum observed hydraulic head map at the QS aquifer. For a better representation of the experiments developed under MARSOL project, the QS model has been converted to a 3D version based on the thickness map calculated by Monteiro *et al.* (2007a) with 6 layers and 7 vertical slices, accounting for a total of 134454 elements and 81641 nodes (Figure 38).

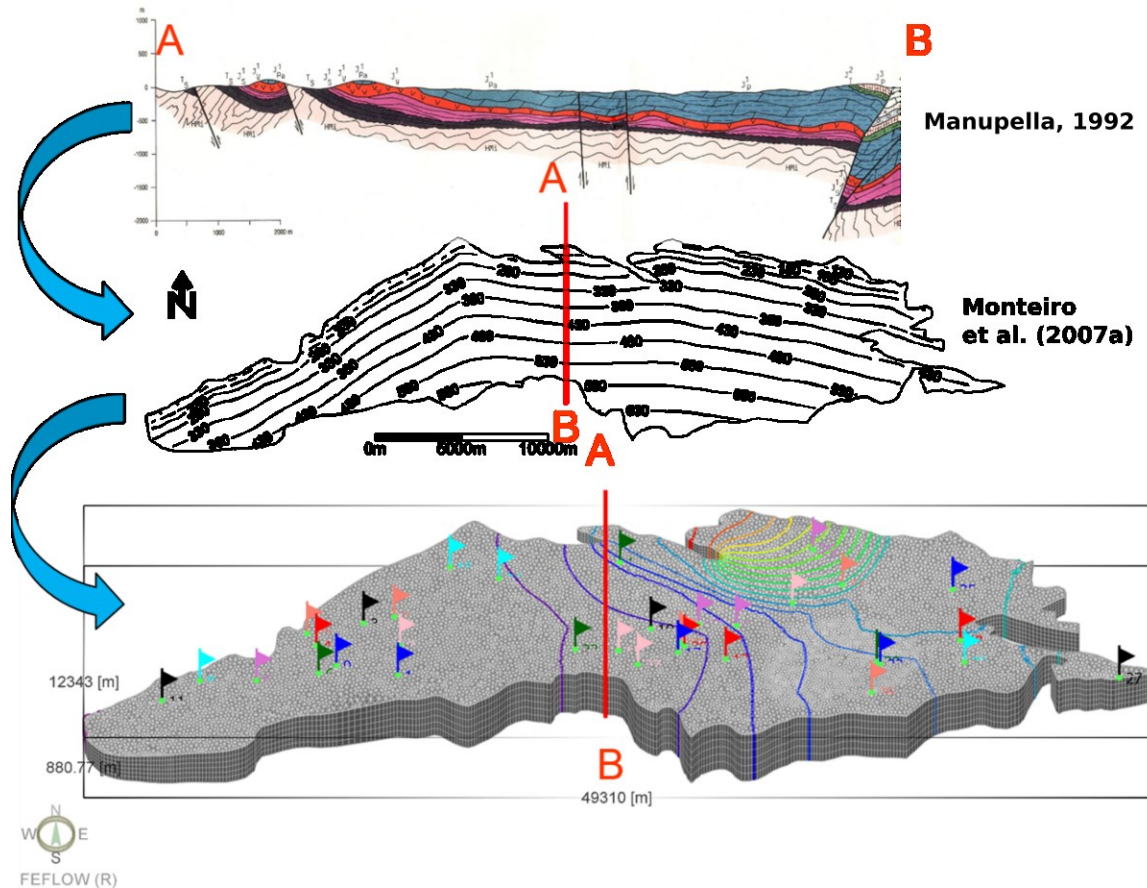


Figure 38 – Development of the 3D geometrical mesh of the Querença-Silves aquifer model

**Numerical model parameters, calibration and boundary conditions**

Previously referred areal recharge rates and estimated average recharge as 45% of rainfall, calculated by Oliveira *et al.* (2011), were imposed in the model. The spatial distribution of the recharge was applied as in Figure 39.

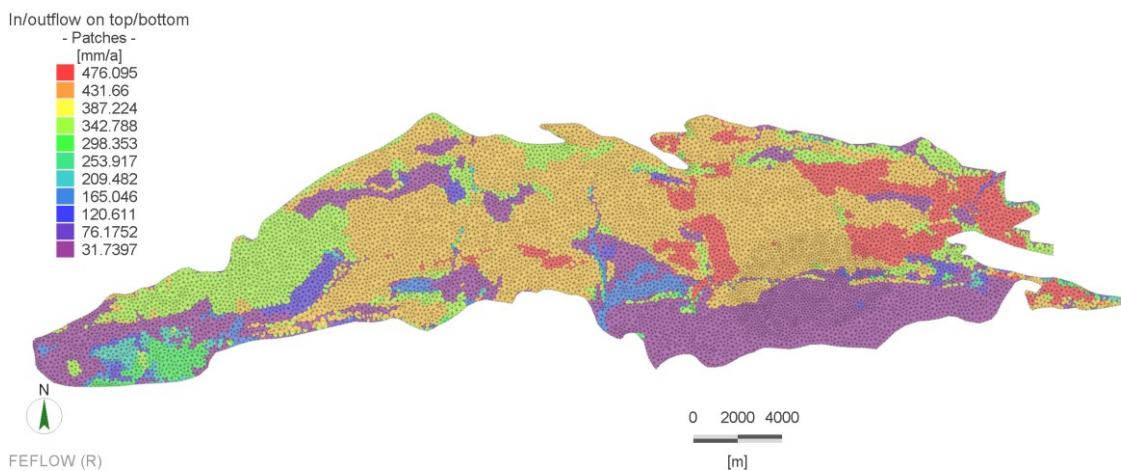
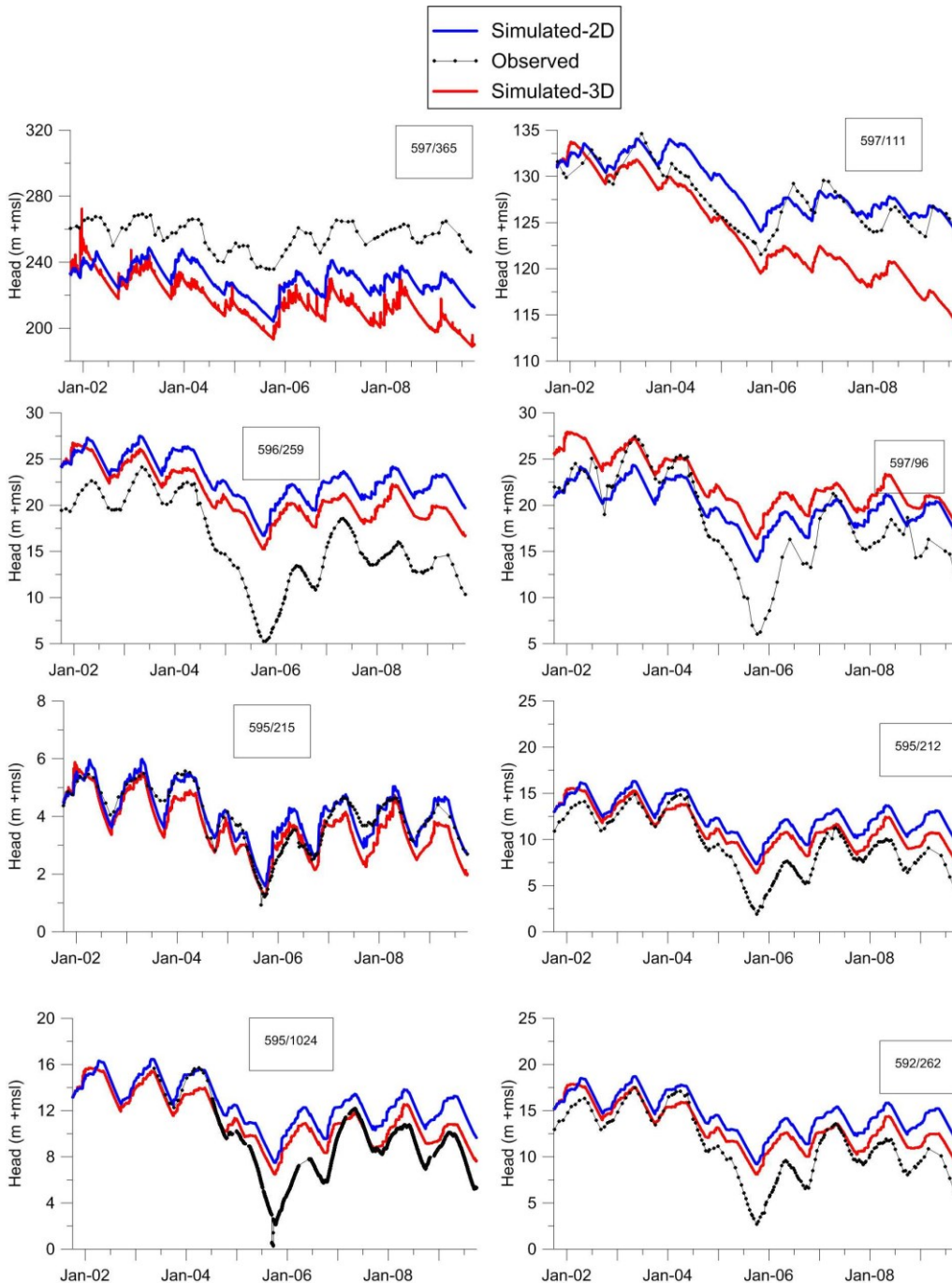


Figure 39 – Average Querença-Silves aquifer recharge (period 1941-1991) as calculated by Oliveira *et al.* (2011)

Hydraulic conductivity at each element was estimated by dividing the calibrated transmissivity for the 2D model by Hugman *et al.* (2012) by the element thickness calculated according to Monteiro *et al.* (2007a). The validation for this calibration is shown in Figure 40 and the resulting hydraulic conductivity distributions is shown in Figure 41.



**Figure 40 – Observed and simulated hydraulic head at several observation wells used to calibrate and validate the Querença–Silves numerical flow model for the 2D and 3D geometry**

Dirichlet boundary conditions were set along the border of the aquifer with the Arade River, with fixed hydraulic head of zero meters, thus simulating aquifer discharge at the Estômbar Springs. Well boundary conditions were defined and imposed on known abstractions located as previously shown on Figure 35, according to extraction scenarios 1 and 2. Private irrigation well abstractions were applied to 150 nodes based on known well locations. The estimated annual abstraction for irrigation was distributed equally among these nodes and under transient conditions for the period of the last week of May to the end of September, as had been previously defined by Hugman *et al.* (2012). Withdrawals for public supply were applied to the nodes corresponding to the Water Utility Águas do Algarve (AdA) wells (Figure 35 and Figure 41) that provided monthly values of abstraction.

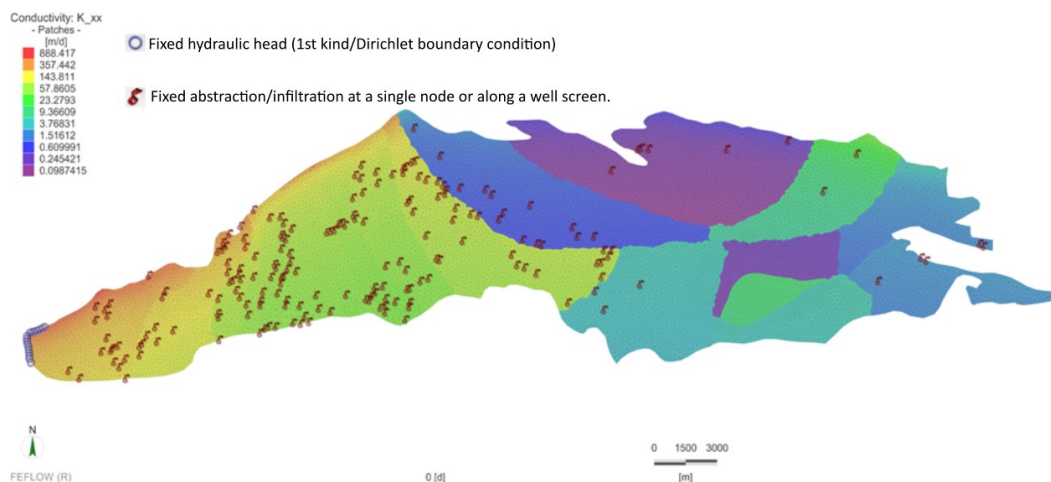


**Figure 41 – Numerical model calibrated hydraulic conductivity distribution and location of Dirichlet boundary conditions and well**

The physical principles of the aquifer system hydraulic behaviour simulation are expressed by the following:

$$S \frac{\partial h}{\partial t} + \text{div}(-[T] \cdot \overrightarrow{\text{grad}} \cdot h) = Q$$

Where  $T$  is transmissivity [ $L^2T^{-1}$ ];  $h$  is the hydraulic head [ $L$ ];  $Q$  is the volumetric flux per unit volume [ $L^3T^{-1}L^{-3}$ ], representing sources and/or sinks; and  $S$  is the storage coefficient [-].

### Modelling scenarios

Two abstraction scenarios were considered for the numerical model (Table 5). Scenario 1 considers water currently exploited by the Water Utility (Águas do Algarve, Lda.) for urban supply, which is  $11.00 \text{ hm}^3/\text{year}$  (Stigter *et al.*, 2009) and for irrigation withdrawals which is estimated as  $30.91 \text{ hm}^3/\text{year}$ , mostly distributed in the western sector of the aquifer (Nunes *et al.*, 2006), performing a total abstracted value of  $42 \text{ hm}^3/\text{year}$ .

Scenario 2 represents the period during which extractions in QS were the most intense in all the historic period of water use in the Algarve region according to the records, corresponding to the drought of 2004-2005. During this period, extraction volumes for municipal urban supply were  $4.6 \text{ hm}^3/\text{year}$  (Silves);  $1.9 \text{ hm}^3/\text{year}$  (Lagoa);  $3.5 \text{ hm}^3/\text{year}$  (Albufeira) and  $0.4 \text{ hm}^3/\text{year}$  (Loulé), which makes a total of  $10.40 \text{ hm}^3/\text{year}$  (Monteiro *et al.*, 2007a; Monteiro *et al.*, 2007b). These values

together with the abstractions from scenario 1 sum up to a total water abstraction value of 52.31 hm<sup>3</sup>/year.

**Table 5 – Abstraction volumes per category for scenario 1 and 2**

	Irrigation (hm <sup>3</sup> /year)	Water Utility (AdA) public supply (hm <sup>3</sup> /year)	Municipal wells for urban supply (hm <sup>3</sup> /year)	Total abstraction (hm <sup>3</sup> /year)
Scenario 1	30.91	11.00	0	41.91
Scenario 2	30.91	11.00	10.40	52.31

For both scenarios, new simulations were performed under steady state conditions, considering the injection of different surface water surplus volumes, ranging from 1 hm<sup>3</sup>/year to 25 hm<sup>3</sup>/year at Cerro do Bardo well and surrounding Water Utility AdA inactive water wells. The aim of this analysis is to determine the resilience of the aquifer towards higher abstractions as were observed during the 2004/05 drought, as well as using surface water surplus from dams in order to mitigate the excess of groundwater explored.

## Results

Results allow estimating the influence of 10 hm<sup>3</sup>/y of MAR with an increase of the hydraulic head upstream the injection area, and the drawback of the saltwater-freshwater interface downstream the injection area (Figure 42). In addition, a saltwater-freshwater sharp interface analysis was performed showing the evolution of the interface at different MAR and abstraction scenarios (

Note: the top image shows the extension of the interface at the bottom of the aquifer. The middle image is a vertical profile representation of the sea water intrusion. The bottom image shows the seawater intrusion plume on a 3D perspective. This example is a simulation of a scenario with the maximum groundwater abstraction recorded at Querença-Silves (period of 2004/2005) without MAR (Figure 43). In this case, the location of the interface was calculated using the Ghyben-Herzberg relation at each node.

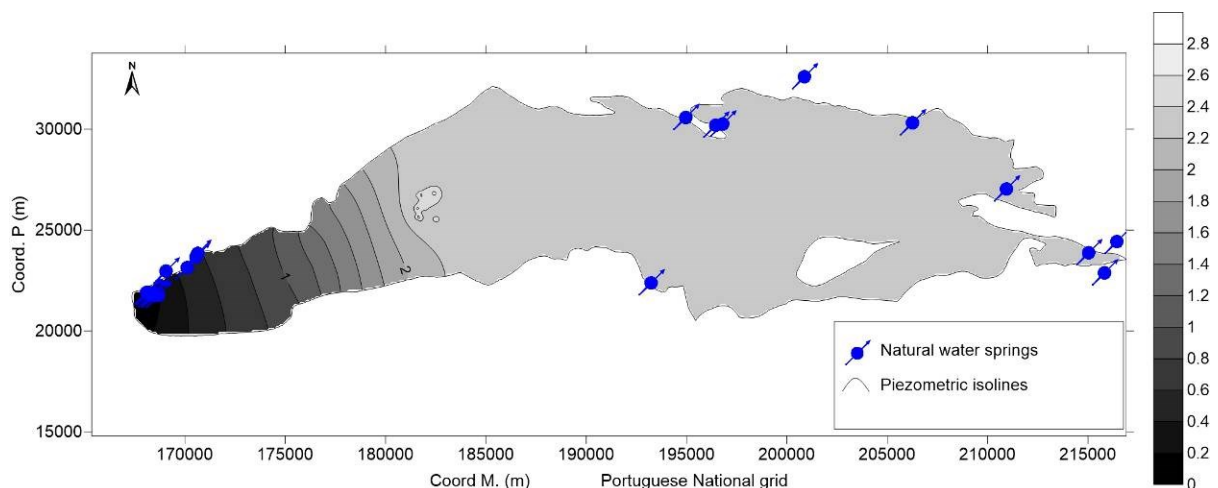
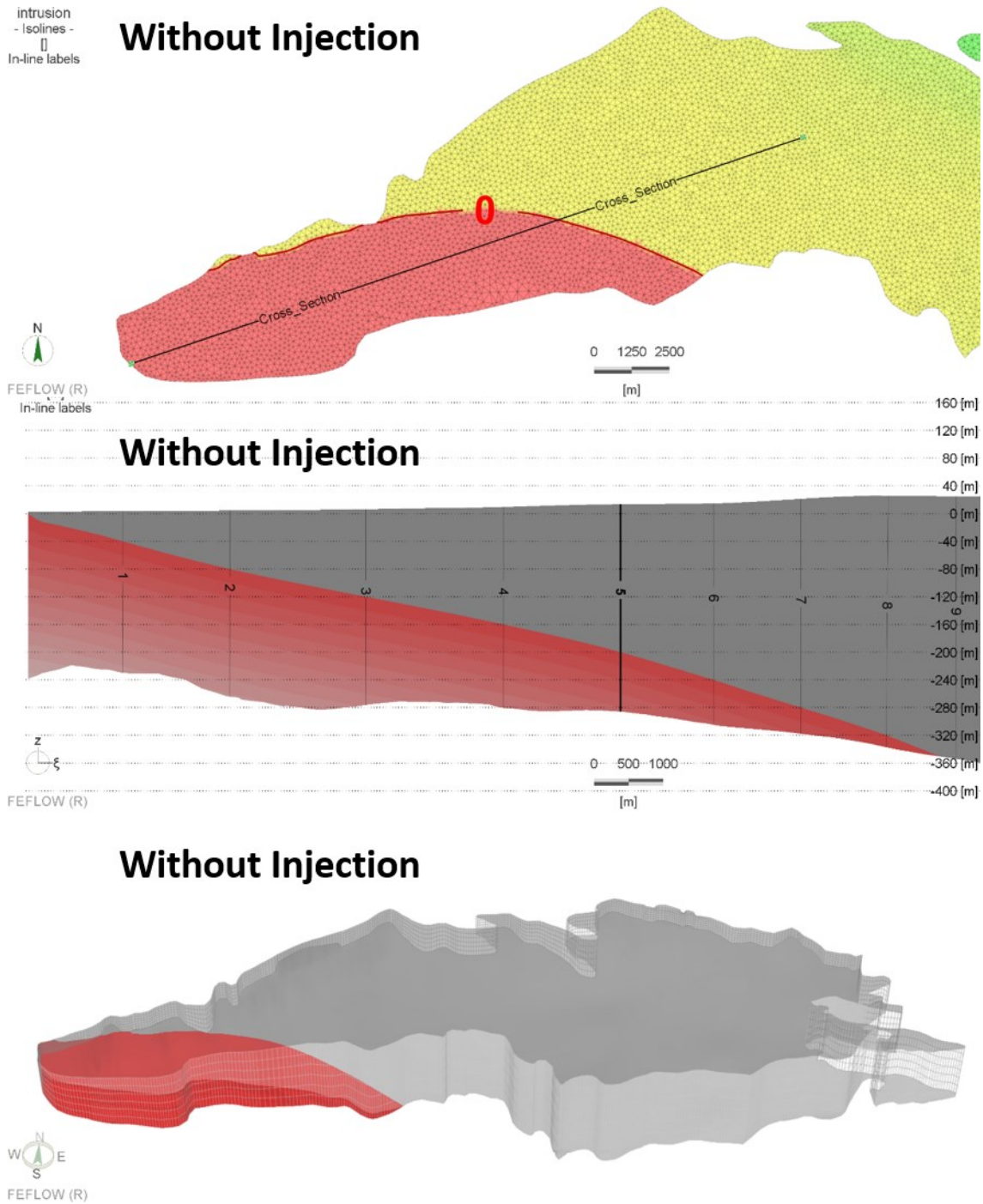


**Figure 42 – Residual between hydraulic head without and with injection of 10 hm<sup>3</sup>/year**





*Note: the top image shows the extension of the interface at the bottom of the aquifer. The middle image is a vertical profile representation of the sea water intrusion. The bottom image shows the seawater intrusion plume on a 3D perspective. This example is a simulation of a scenario with the maximum groundwater abstraction recorded at Querença-Silves (period of 2004/2005) without MAR*

**Figure 43 – Sharp interface analysis of saltwater-freshwater interface at Querença-Silves.**

Considering the know-how developed during MARSOL project, the most feasible MAR scenario at Querença-Silves (based on water availability and existing infrastructures infiltration capacity) would

consist of injecting  $3 \text{ hm}^3/\text{year}$  under scenario 1 conditions, i.e. current groundwater abstraction. The model simulation results for this scenario are presented in Figure 44, which shows the residual hydraulic head between business as usual and injecting  $3 \text{ hm}^3/\text{year}$  at Cerro do Bardo, or in other words, the resulting increase in groundwater level upon injecting  $3 \text{ hm}^3/\text{year}$ .

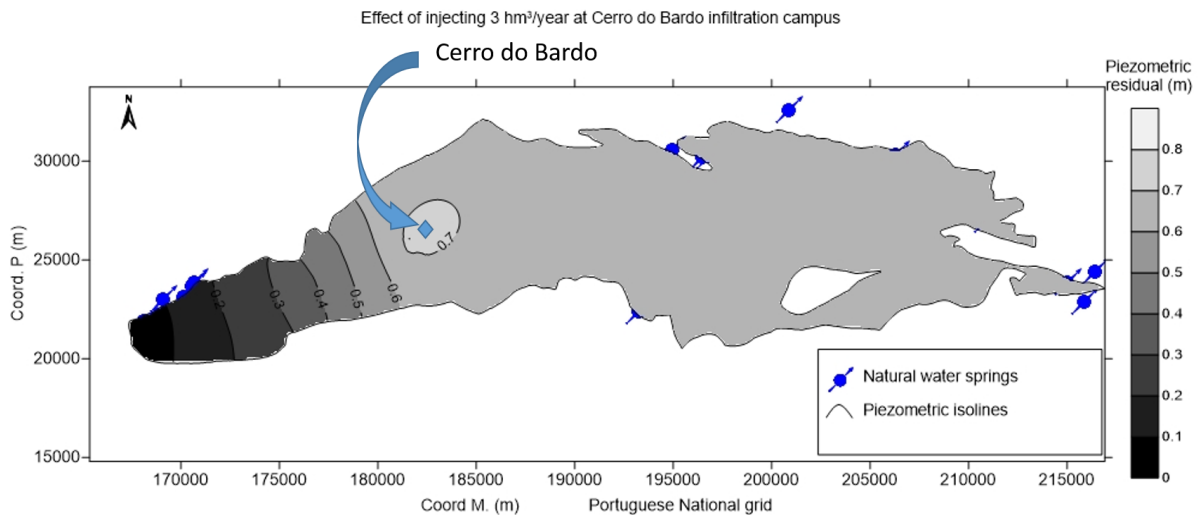


**Figure 44 – Residual between hydraulic head without and with injection of  $3 \text{ hm}^3/\text{year}$**

Modelling shows that a very impressive effect can be observed upstream of the MAR facilities, due to its barrier effect with the general flow, resulting in an increase in groundwater level of about 0.6 to 0.7 m in most of the aquifer. Also, MAR activities might mitigate and avoid further saltwater intrusion in the Arade river estuary. By applying a sharp interface approach based on Ghyben-Herzberg principle it is possible to obtain rough estimates on the total affected area by the seawater intrusion. Considering business as usual, a total volume of  $22.43 \text{ km}^3$  at the aquifer model are being affected by seawater intrusion. On the other hand, when injecting  $3 \text{ hm}^3/\text{year}$  the volume of the aquifer model affected by seawater intrusion decreases to  $20.24 \text{ km}^3$ . Hence, a total volume of  $2.13 \text{ km}^3$  of aquifer in the water front can be relieved from seawater intrusion by injecting  $3 \text{ hm}^3/\text{year}$ .

#### Local scale analysis at Querença-Silves

Parallel to the previous efforts, the same model was also used to simulate the influence of the local scale injection at Cerro do Bardo (CB) large diameter well on April 1<sup>st</sup>, 2014. The interpretation of this injection test is depicted in MARSOL deliverables 4.3 and 4.2. It consisted of an injection test at CB well (with a depth of 32 meters and a diameter of 2 meters). In order to obtain early estimates for the well infiltration rate capacity, an infiltration test with a flow of  $125.20 \text{ m}^3/\text{h}$  and  $40 \text{ m}^3$  of water was performed on the well (during approximately 19 minutes). The injection of water has produced a maximum water rise of 6.38 m though stabilization of the water level has not been achieved. Table 6 summarizes the estimated infiltration rate for the recovery period of the injection test.

**Table 6 – Results of the recovery period from the injection test. Water displacement and infiltration rate**

Time (hours)	1	2	3	4	5	6	7
$\Delta h$ (m)	3.28	0.88	0.51	0.36	0.26	0.18	0.14
Infiltration rate (m/d)	78.82	21.17	12.22	8.52	6.26	4.3	3.26

As can be seen from Figure 45, results indicate an expected relation between the infiltration rate and the hydraulic load in the well (i.e. water level in the well).

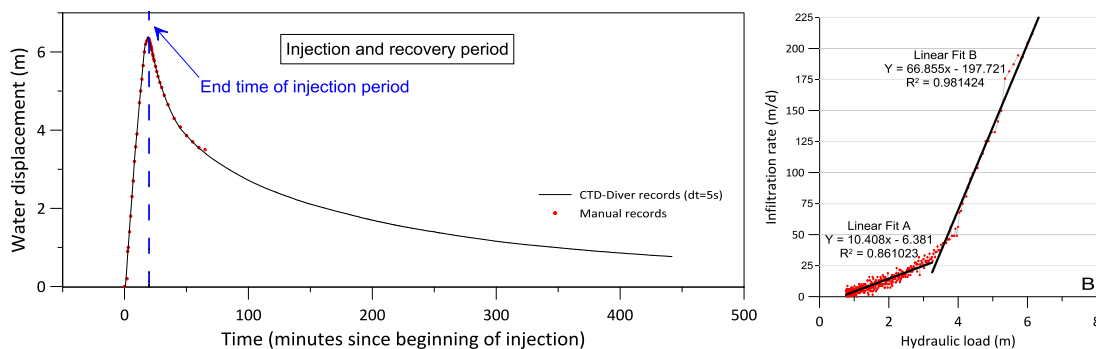


**Figure 45 – LEFT: Records for water displacement in the well as a function of time. RIGHT: Scatter plot between hydraulic load and infiltration rate and its linear fits**

Two different phases can be evidenced from Figure 45-Right in the relation between the infiltration rate and the hydraulic load. The first one is set by lower hydraulic load (up to around 3.25 m), in which infiltration rate can reach up to 25 m/d. The second phase, for higher hydraulic loads (above 3.25 m) originates infiltration rates higher than 25 m/d, reaching, in this test, a maximum of 211 m/d, at 6.35 m. The two linear fits identified could possibly be associated with the existence of a double porosity system, to the wellbore storage, or to existing infiltrating conditions inside the well above 3.25 m displacement elevation.

The numerical modelling efforts results show that the simulated hydraulic response of the aquifer with the regional model underestimate the observed behaviour monitored at the scale of the well. This happens mainly due to the characteristics of well among other factors, like the element size of the mesh around the well.

As can be seen on Figure 46 by refining the mesh node density, and thus, decreasing the element size, the calculated hydraulic head error decreases. Yet, a rather dense mesh than the ones presented here would be necessary to effectively reach a calculated hydraulic head similar to the observed during the injection test.

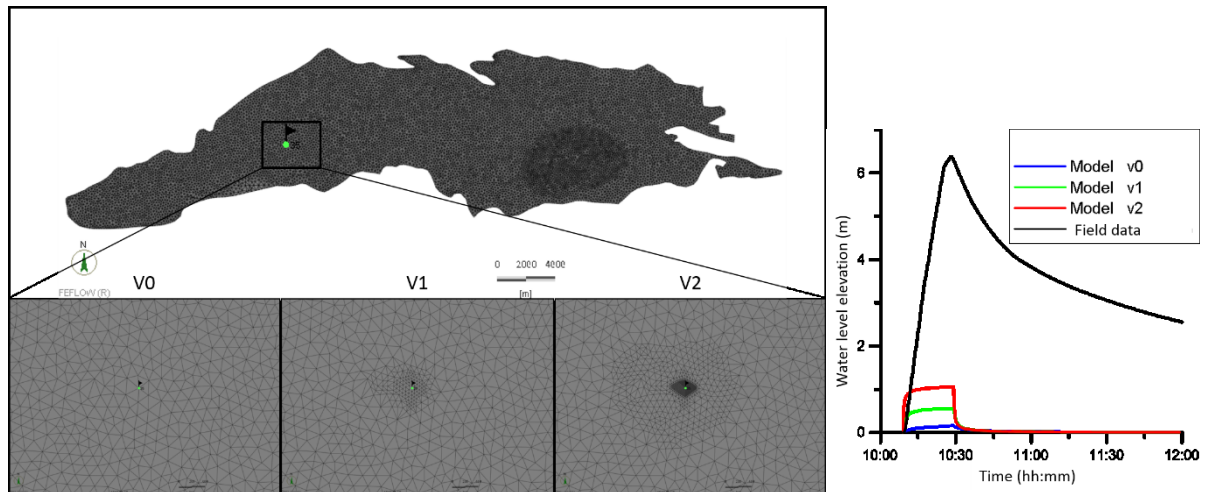


Figure 46 – Effect of mesh density on simulated hydraulic head during injection test

In this case, the use of analytical solutions of well hydraulics consists of a more suitable approach in order to determine the hydraulic properties controlling the flow in the well, as well as for representing the observed hydraulic heads in the well. Costa *et al.* (2015) presents an analysis on an injection test performed at Cerro do Bardo under MARSOL project, in which an analytical model was used in order to represent the hydraulic head behaviour in the well, as well as to determine the hydraulic properties at the well local scale.

Detailed insight and methodologies on analytical solution methods for different configuration pumping tests can be found in bibliography. Injection tests are considered conceptually identical to pumping tests, except that flow is into the well rather than out of it (Horne, 1990; Kruseman *et al.*, 1990). Notwithstanding, there is generally a tendency to increase hydraulic conductivity when extracting and to decrease hydraulic conductivity during injection. Extraction removes fines whereas injection may create clogging.

In order to better understand the factors controlling the infiltration of water in the well into the aquifer and estimate aquifer parameters (transmissivity and storage) and well parameters (storage and skin factor), an aquifer parameter analysis was performed with the support of the aquifer test analysis software MLU version 2.25.63 (Hemker & Post, 2014), which consists of an analytical groundwater modelling tool to compute drawdowns, analyse well flow and aquifer test data based on a single analytical solution technique for well flow. Due to the high level of uncertainty regarding both the aquifer and the well configuration, a sensitivity analysis was performed, considering several possible aquifer and well configurations.

From the sensitivity analysis, transmissivity values were found ranging from 14.99 to 36.64 m<sup>2</sup>/day and storage coefficient from 7.09x10<sup>-02</sup> to 6.38x10<sup>-1</sup>. The configuration that better appears to represent the reality is the one which considers the well is installed on an upper unconfined aquifer (thickness 10.75 m) separated by the regional aquifer by an implicit aquitard. For this configuration, transmissivity for the top layer is estimated as 14.99 m<sup>2</sup>/d. Figure 47 shows the correlation between the observed and calculated drawdown data of the injection test for this configuration.

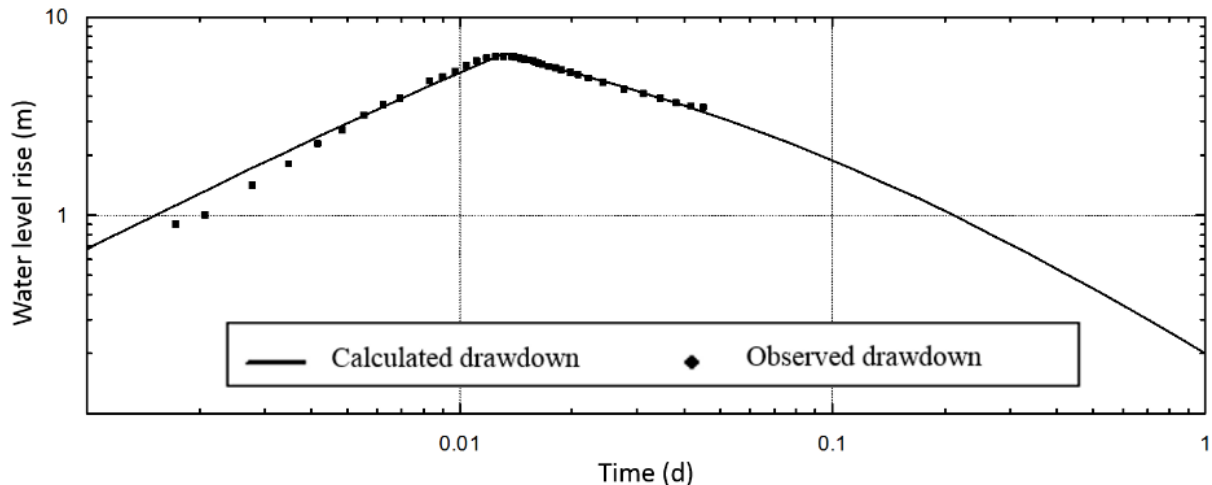


**Figure 47 – Comparison of observed and calculated data based on optimized values of aquifer parameters**

There lies a high degree of uncertainty regarding the Cerro do Bardo well characteristics, the local aquifer geometry and the connection between the well and the aquifer. On one hand, the information supplied by the local inhabitants suggests that flow in the area is from West to East, opposing to the regional flow. Also, it appears there is a confining or lower permeability layer at around 30 to 40 meters depth, which coincides with the Cerro do Bardo wells depth. This probably means the well is not in direct contact with the regional aquifer or any of its karst conduits. On the other hand, parameter estimation during the injection test at the well returned transmissivity values much lower than the average transmissivity values determined by previous pumping tests in the surrounding (and much deeper) wells. This fact also indicates that Cerro do Bardo well isn't directly linked with the regional aquifer.

With the support of MLU software several possible aquifer and well configurations were simulated, achieving transmissivity values ranging from 14.99 to 36.64 m<sup>2</sup>/d. Although the results obtained from the analytical models for interpreting pumping tests suggest Cerro do Bardo well is locally separated from the regional aquifer by an implicit local aquitard or a confining layer, the non-uniqueness of the factors contributing for the observed hydraulic responses, as well as geophysics experimental results gathered by LNEC at the test site, raises doubts related to the non-connectivity in localized areas. In these areas the regional aquifer and the top aquifer would be in direct contact. If this is the case, then the MAR into the well would be directly incorporated in the regional aquifer, for later use down-gradient.

## 2.2.6 Numerical modelling of soil-column experiments at LNEC

### Introduction

Numerical modelling exercises were conducted using data collected in the soil-column experiments. These exercises represented a helpful tool to describe contaminants behaviour as well as some removal mechanisms and the conditions in which they occur. Solute transport was considered for the column behaviour understanding.



A set of soil-column experiments were conducted in MARSOL (see Work Package 14 concerning water quality where water constituents, fate of pollutants and soil column experiments were studied) using the natural soil of the area of installation of the infiltration basins in the South of Portugal DEMO area of São Bartolomeu de Messines in the Querença – Silves aquifer system.

The soil-column experiments apparatus used is briefly presented in Figure 48. In this apparatus two types of injection can be considered – continuous or by pulse. For continuous water injection, a volumetric peristaltic pump is used while for pulse injection the water was directly poured from a container to the column. Water naturally flows from the bottom outlet to the sample tubes and outflow samples were collected at defined periods and conditioned in dark glass vials or bottles for later analysis.

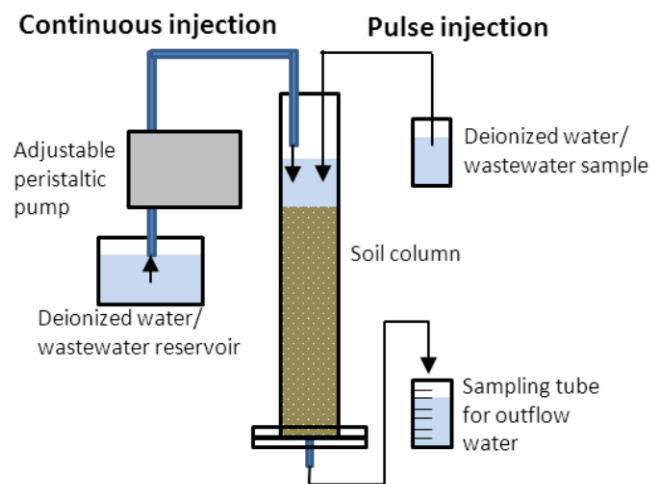


**Figure 48 – Soil-column apparatus and diagram of operation**

Besides the natural soil of the area of installation, water that will be used in real scale facilities was also used in the experiments - wastewater was collected in São Bartolomeu de Messines Wastewater Treatment Plant for previous injection in the columns of soil. Both soil and water were characterized concerning constitution and quality. The soil characterization and inflow wastewater quality results are presented in Martins (2016). The experiments were held in different time periods, from a few hours to several days and aimed to assess the importance of soil compaction procedures, saturation-desaturation processes and the effects of inflow water quality can have in the outflow rate. In total 5 soil-column experiments were conducted in the natural soil. Table 7 presents the main characteristics of the soil-column experiments which results were considered in the modelling process (Column 3 and Column 4).

**Table 7 – Synthesis of the operating details of the soil-column experiments conducted in the natural soil**

	<b>Column 3</b>	<b>Column 4</b>
Soil thickness (cm)	20	30
Saturation conditions	Started saturated Always saturated	Started saturated Unsaturated/ saturated cycles
Injection method	Continuous	Continuous/ pulse
Experiment time length (days)	5	33

For the solute transport modelling Hydrus-1D (Jacques and Šimůnek, 2005) was used. This software is widely used to simulate flow and solute transport in variably saturated soils and groundwater in both steady and transient state. One dimensional flow can be modelled at different scales from laboratory soil-columns to larger experiments. Hydrus-1D can also considerer inverse problems when some parameters need to be calibrated or estimated from observed data.

### Input data

Given that nitrogen cycle is highly dependent on redox conditions, modelling the nitrification process can be useful to understand the conditions inside the column. Also, nitrogen cycle constituents are common in the matrix of the water injected in the columns – treated wastewater.

For this modelling process only continuous saturated conditions were considered – all time length of Column 3 experiment (continuous flow) and the first saturation cycle of Column 4. Other soil-column experiments results were not considered due to the small number of outflow samples or because short sat-unsaturation cycles used where no samples were collected.

Concerning the contaminants which transport was modelled, three main compounds were considered – nitrates (NO<sub>3</sub>), nitrites (NO<sub>2</sub>) and ammonia (NH<sub>4</sub>). The concentrations measured both at inflow and outflow are presented in Figure 49 (Column 3) and Figure 50 (Column 4).

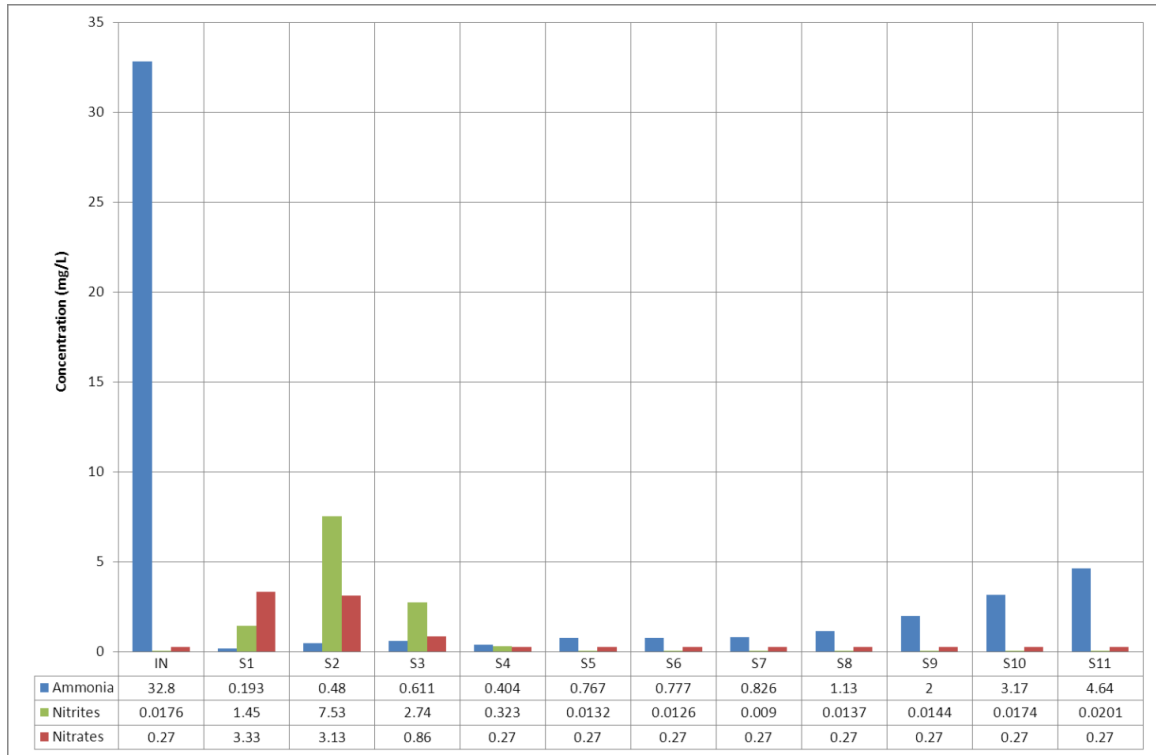


Figure 49 – Nitrogen cycle components concentration in Column 3 inflow/outflow

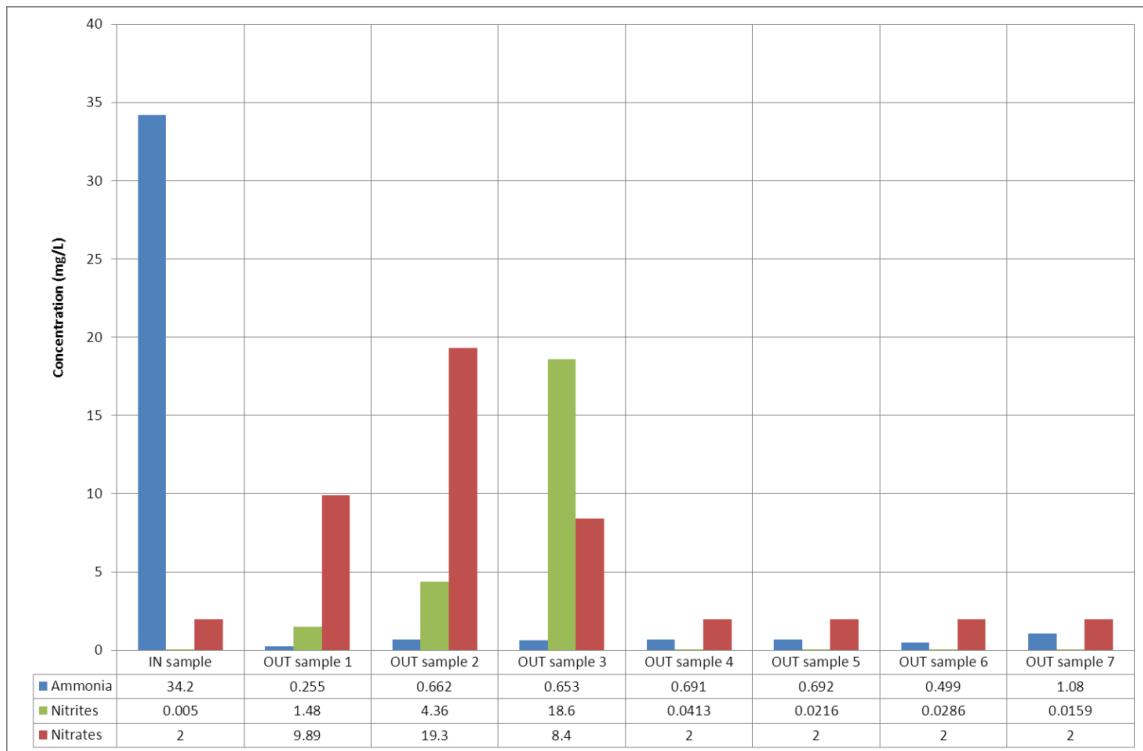


Figure 50 – Nitrogen cycle components concentration in Column 4 inflow/outflow

Simulations were run in transient state for solute transport, where the inflow and outflow concentrations were considered as solute top and bottom boundary conditions respectively. Both models were divided into five time intervals.

Input parameters for both soil-column experiments are presented in Table 8. Some of the input parameters were obtained by bibliographic research while others were inverse modelled (Ilie, 2015).

**Table 8 – Input data for Hydrus-1D C3 and C4 models.**

Parameter		Column 3	Column 4	Ref.	Observations
Depth of the soil profile (cm)		20	30	-	-
Total time (min)		6131	3084	-	-
Time-variable boundary conditions		12	8	-	-
Soil parameters	Bulk density (g/cm <sup>3</sup> )	1.44	1.52	Ilie (2015)	Determined by Rosetta Lite v1.1 from soil granulometry without considering > 2 mm fraction (clay = 78.51%; silt = 18.96%; sand = 2.53%)
	Qr	0.0368	0.0364		
	Qs	0.3907	0.3704		
	Alpha (1/cm)	0.0446	0.0457		
	n	1.7305	1.7596		
	Ks (cm/min)	0.1011	0.0798		
Boundary condition	Upper	Constant pressure head (20 cm)	Constant pressure head (30 cm)	-	-
	Lower	Free drainage		-	-
Solute parameters	Long. Dispersivity	2	2	Simunek <i>et al.</i> (2013)	-
	Diffus. Water.	0.000833	0.000833	Ramos and Carbonell (1991)	-
	Reaction parameters	Inverse solution modelling		Ilie (2015)	-
Solute transport boundary cond.	Upper	Concentration flux BC		-	-
	Lower	Zero concentration gradient		-	-

## Results

Simulations were successful and the model converged to a solution. Model results of contaminant concentration vs depth for both columns for the solutes are presented in Figure 51.

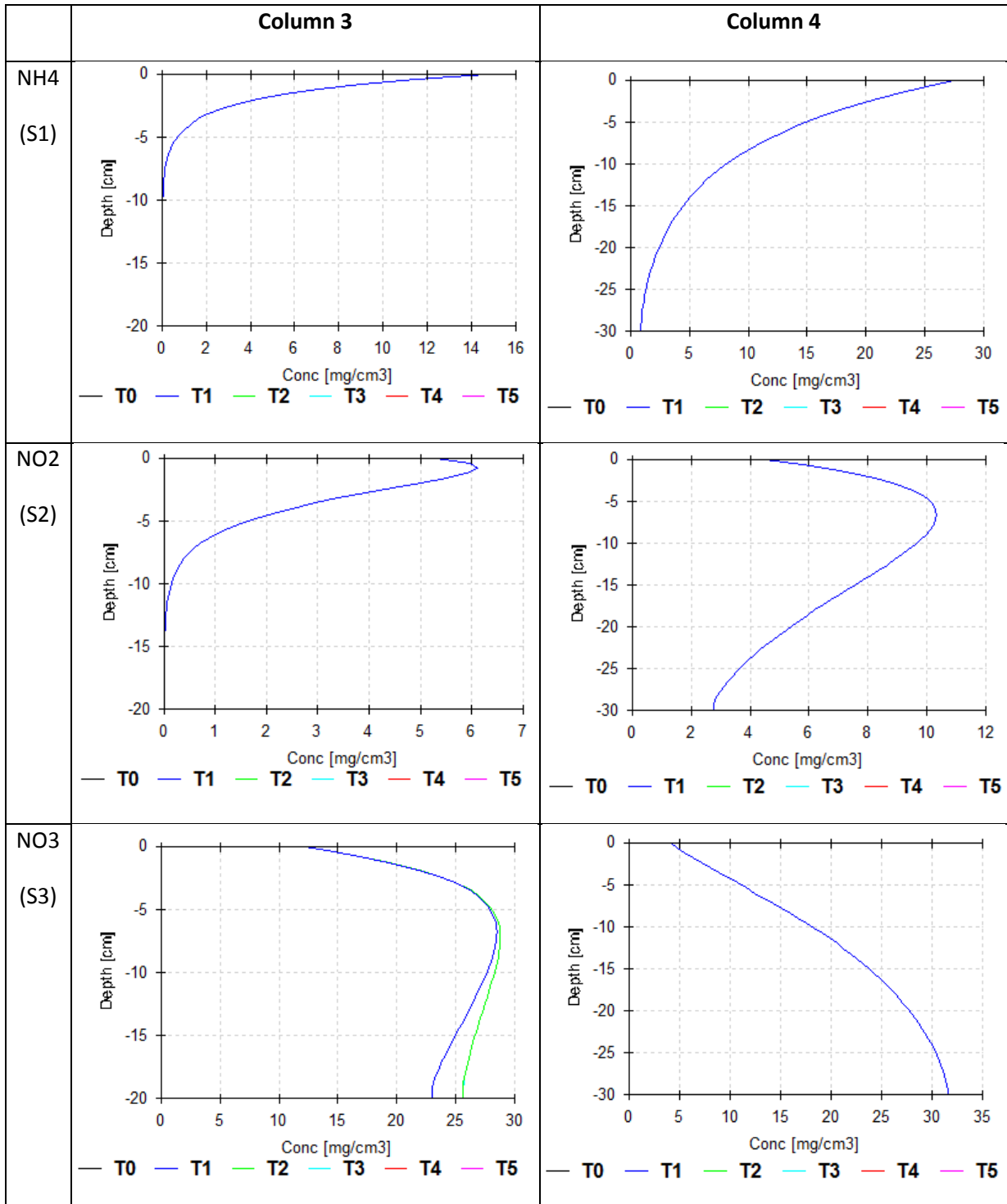
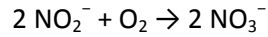
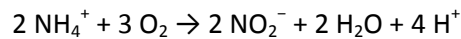


Figure 51 – Hydrus-1D results for nitrogen simulation (concentration through depth)

Both simulations show similar behaviour along the columns, with ammonia being mostly retained on the top of the column whereas nitrites show a small increase in concentration as ammonia is oxidized to nitrite, and then nitrites decrease at the column bottom as they are transformed into nitrates. This confirms that nitrification may be expected in soil-columns confirming, from the



analysis of the results of the three columns, that ammonia ( $\text{NH}_4^+$ ) is being nitrified while nitrites ( $\text{NO}_2^-$ ) and nitrates ( $\text{NO}_3^-$ ) concentration increased:



In Column 3 simulation, ammonia concentration rapidly decreases to zero at the first half of the column while in Column 4 some ammonia can be observed at the bottom section but in much lower concentration than that observed on the top. Nitrites concentrations show a small increase in the first centimetres of the column top and decreases again. In Column 4 bottom nitrites are observed at the outflow. Nitrates continuously increase in Column 4 while in Column 3 this compound increases at the first  $\frac{1}{4}$  of the column thickness and slowly decreases after that.

For the considered parameters, solute retention and possibly transformation can be observed, which can suggest that good conditions occur at the columns for nitrification, with lower oxygen content on the column top as water is injected and slight oxygenation on the bottom (where higher concentration of nitrates is observed).

Five nodes were represented along both columns, equally distributed between them. Results for variation of concentration through time taken from these nodes (from top to bottom) are presented in Figure 52 and Figure 53.

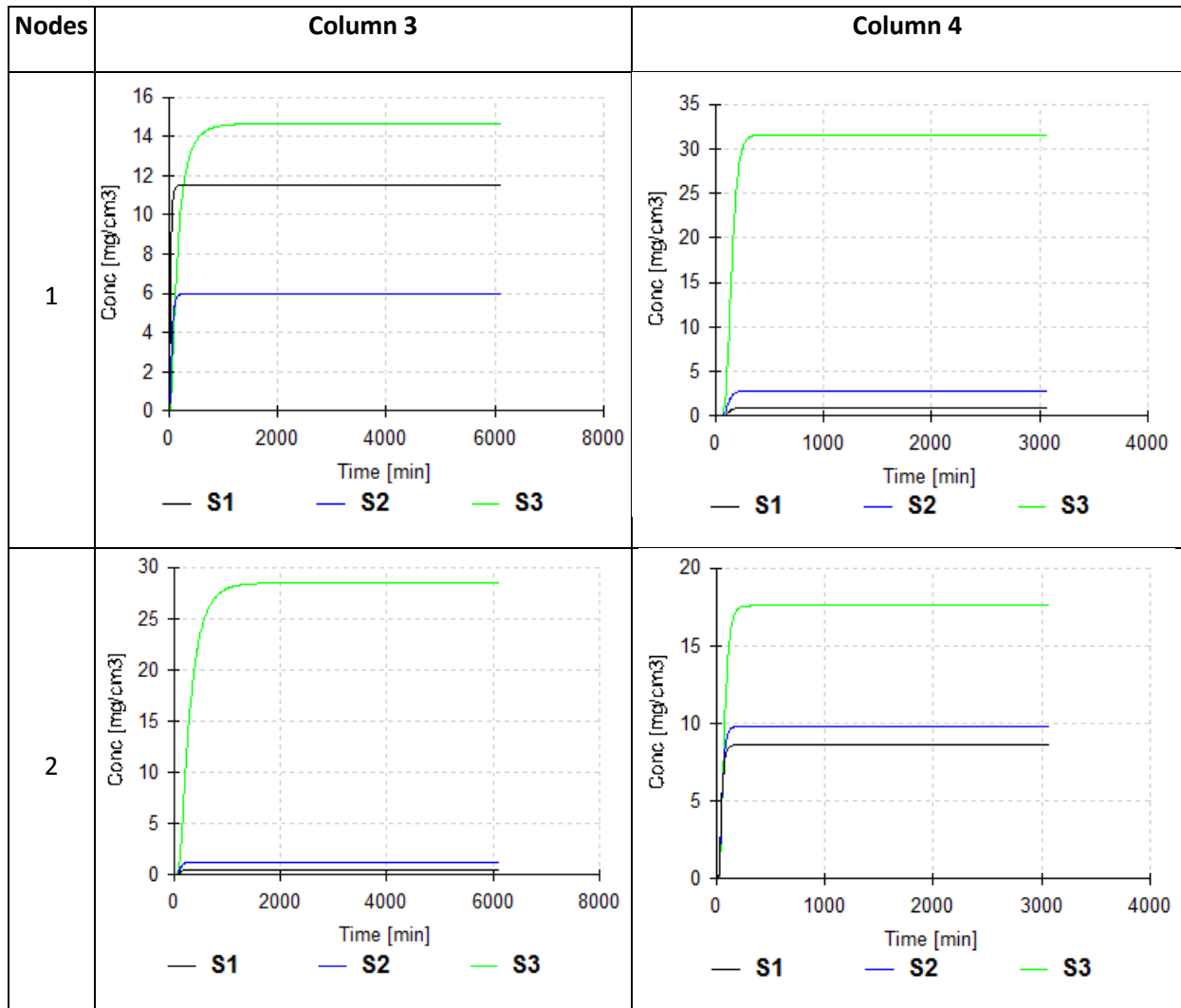


Figure 52 – Hydrus-1D results for nitrogen simulation for node 1 and 2 (S1 – ammonia, S2 – nitrites, S3 – nitrates)

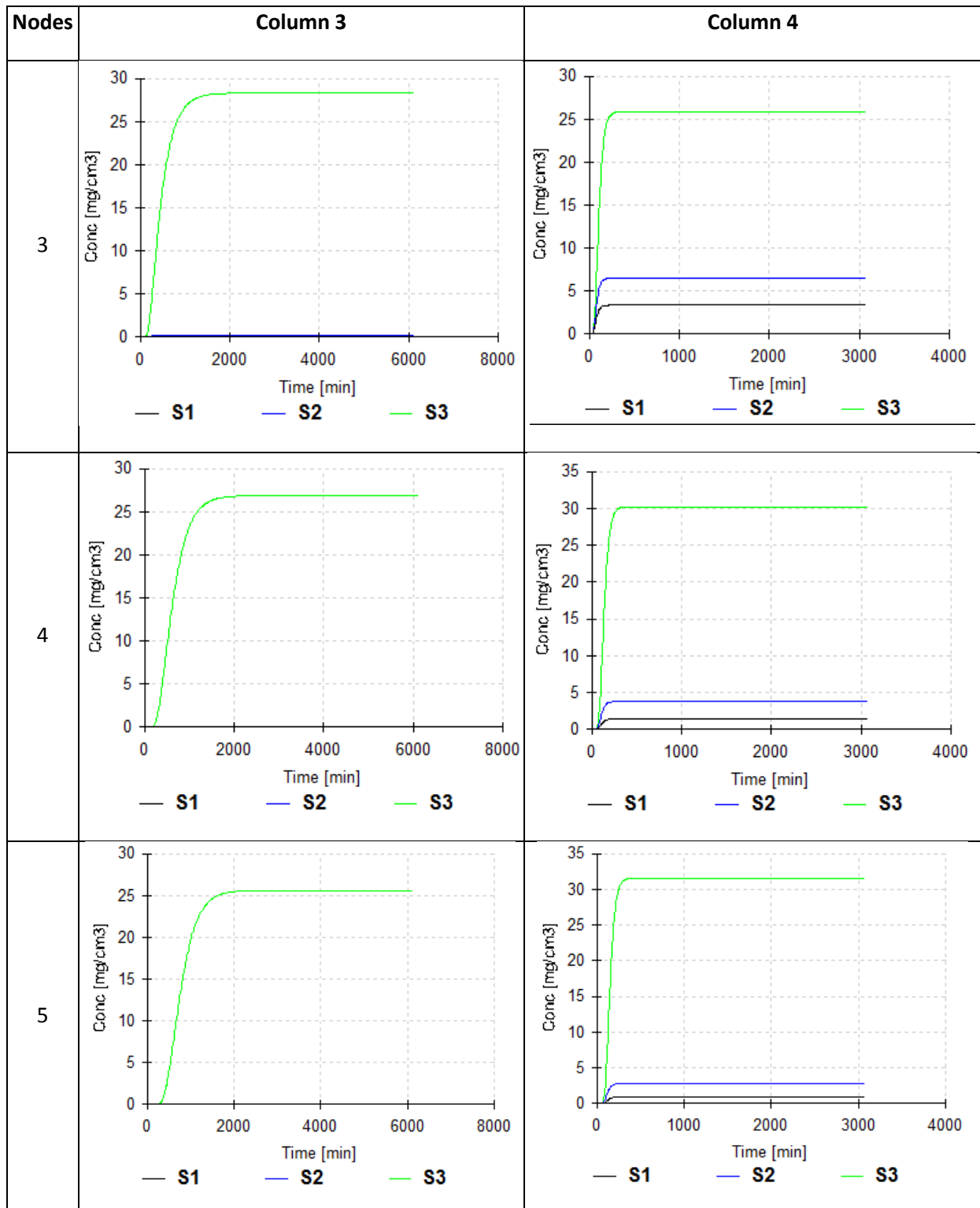


Figure 53 – Hydrus-1D results for nitrogen simulation for nodes 3, 4 and 5 (S1 – ammonia, S2 – nitrites, S3 – nitrates)

Solute behaviour is observed in different depths along the columns, through time (from point 1 to 5). Again ammonia (S1) concentrations are very low (or null) at the bottom in both columns.

In an overview of the model results, Column 3 achieves stabilization in these compounds concentration in the first 1000 minutes and in Column 4 at approximately 200 minutes. If pore-volumes determined in soil-column experiments are considered and that 1L of water is injected in both columns (steady state flow), these periods correspond to 5.7PV for C3 and 3.8PV for C4.

### **Discussion and conclusions**

Although ammonia retention on the column is confirmed by inflow and outflow comparison, particularly in natural soil experiments, the observed behaviour calculated in simulations is not what is observed in the soil-column experiments results, considering nitrates concentration. In soil-columns, nitrates show low concentration at outflow, instead of high concentrations calculated in the model. This may result from the time of simulation considered, but also, in the soil columns, to a process of retention of nitrates, observed in the models, where nitrates have high concentrations at the bottom section of the column and possibly are not mobilized to the water. These models can be calibrated for future experiments, but this simple approach of soil-column modelling allowed understanding and predicting the behaviour of a set of contaminants.

## 2.3 PT3: MELIDES AQUIFER, RIVER AND LAGOON (ALENTEJO)

### 2.3.1 LNEC physical sandbox model

In PT3 it was decided that the planned water quality control would be made using a SAT-MAR prototype basin not placed *in situ* but at a large laboratory scale on a physical (sandbox) model at LNEC (Figure 54).



Figure 54 – LNEC Physical (sandbox) model construction

This sandbox model was divided into three sections (Figure 55) to test the adsorption and degradation capacity of three different soil mixtures. Figure 56 presents a schematic diagram of the sandbox model dimensions.



Figure 55 – LNEC physical (sandbox) model sections, A, B and C



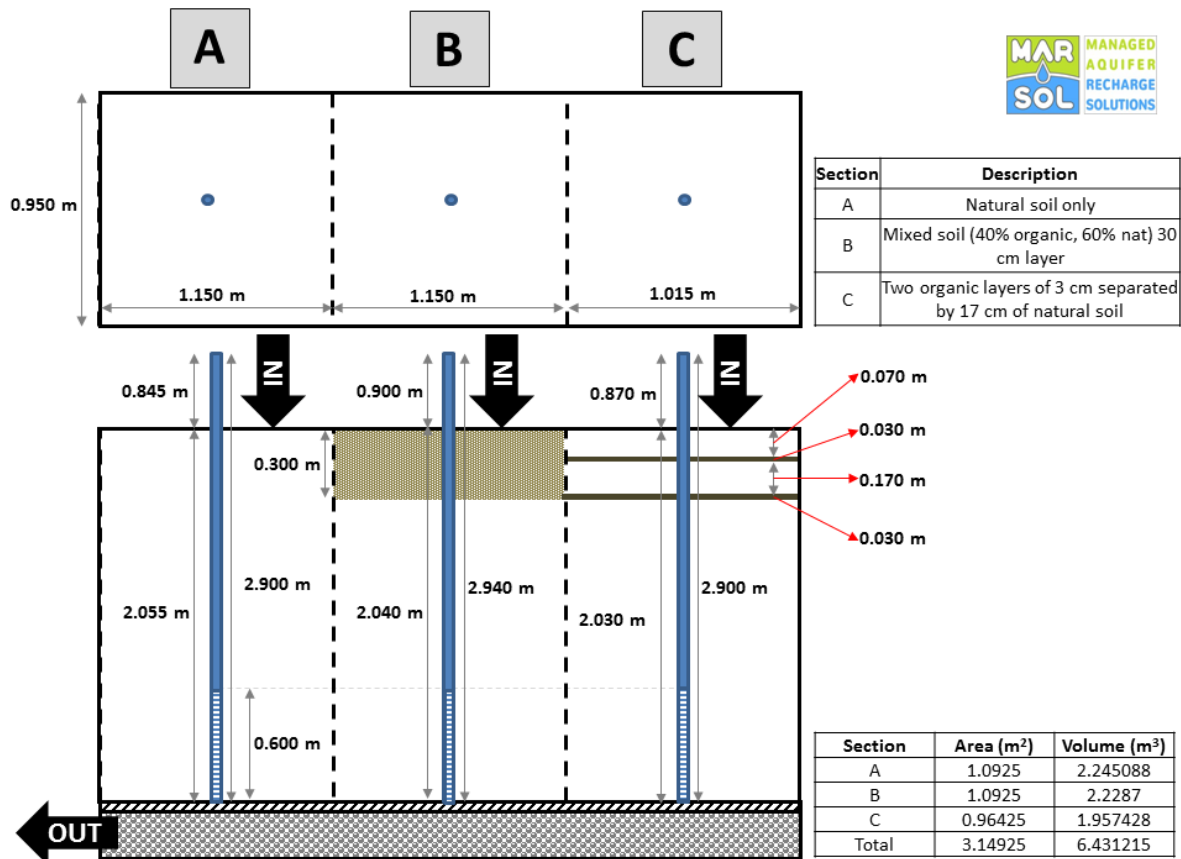


Figure 56 – Schematic diagram of the physical (sandbox) model dimensions

### 2.3.2 Investigation experiments and monitoring

Considering the results from the soil-column experiments conducted at LNEC LASUB facilities in May and June 2014 to determine the hydraulic characteristics of the Melides soils (from a depth of 5 to 20 and 20 to 30 cm layers at the approximate location of the infiltration site), it was concluded that the soil has a permeability value adequate for SAT, with an average Darcy permeability ranging from 0,9 to 4,8 m/d at Melides, the latter for a 20-30 cm layer where permeability increase significantly.

Melides soil was acquired and used to fill the sandbox model, accordingly to the scheme presented in Figure 56.

Two spiked tracer experiments, with fertilizers and hydrocarbons, were done in May/June 2016. In those experiments it was assessed the:

- Water infiltration capacity.
- Water quality in the vadose zone, at two depths, 30 cm and 60 cm, using Prenart capsules to access SAT treatment.
- Water quality in the saturated zone (*in situ*: T, EC, pH, redox; chemical parameters).
- Soil at 30 cm and 60 cm.

These results will be further developed under WP12, Task 12.5 and will be reported in D12.5.

## REFERENCES

- Costa L, Monteiro JP, Oliveira MM, et al (2015) Interpretation of an Injection Test in a Large Diameter Well in South Portugal and Contribution to the Understanding of the Local Hydrogeology. In: 10<sup>o</sup> Seminário de Águas Subterrâneas - Associação Portuguesa de Recursos Hídricos (APRH). Universidade de Évora, 9 e 10 de Abril de 2015, Évora. pp 61–64.
- Diamantino Roseiro C (2009) Recarga artificial de aquíferos: aplicação ao sistema aquífero da Campina de Faro. Tese de Doutoramento. FCUL.
- Hemker CJ, Post V (2014) MLU for Windows. Well flow modeling in multilayer aquifer systems. MLU Users Guide, 2014. Available at [www.microfem.com](http://www.microfem.com).
- Horne RN (1990) Modern Well Test Analysis: A Computer-Aided Approach. Petroway Inc., Palo Alto, USA, 185.
- Hugman R, Stigter TY, Monteiro JP, Nunes L (2012) Influence of aquifer properties and the spatial and temporal distribution of recharge and abstraction on sustainable yields in semi-arid regions. *Hydrol Process* 26:2791–2801. doi: 10.1002/hyp.8353.
- Hugman R, Stigter TY, Monteiro JP (2013) The importance of temporal scale when optimising abstraction volumes for sustainable aquifer exploitation: A case study in semi-arid South Portugal. *J Hydrol* 490:1–10. doi: 10.1016/j.jhydrol.2013.02.053
- Ilie, A.M. (2015) Personal communication.
- Jacques, D., Šimůnek, J. (2005) User Manual of the Multicomponent Variably-Saturated Flow and Transport Model HP1, Description, Verification and Examples, Version 1.0, SCK/CEN-BLG-998, Waste and Disposal, SCK/CEN, 79 pp.
- Kruseman GP, De Ridder NA, Verweij JM (1990) Analysis and evaluation of pumping test data (2nd ed.). International Institute for Land Reclamation, 377p.
- Leitão TE, Lobo Ferreira JP, Oliveira MM, Martins T, Henriques MJ, Mota R, Carvalho TM, Martins de Carvalho J, Agostinho R, Carvalho R, Sousa R, Monteiro JP, Costa LRD e HUGMAN R 2016 – Deliverable 4.3 Monitoring Results from the South Portugal MARSOL Demonstration Sites. UE MARSOL project - Demonstrating Managed Aquifer Recharge as a Solution to Water Scarcity and Drought, July, 118 pp.
- Lobo-Ferreira JP, Diamantino C, Moinante M, et al (2006) Groundwater artificial recharge based on alternative sources of water : advanced integrated technologies and management. Deliverable D51 – Test sites and their characteristics (Month 12).
- MANUPELLA G (1992) Notícia Explicativa da Carta geológica da região do Algarve (escala 1/100000) [Explanatory note of geological map of the Algarve region].
- Martins, T. (2016) Contaminants retention in soils as a complementary water treatment method: application in soil-aquifer treatment processes. Master Thesis. Faculty of Sciences. University of Lisbon, 2016.
- Monteiro JP, Ribeiro L, Martins J (2007a) Modelação Matemática do Sistema Aquífero Querença-Silves. Validação e Análise de Cenários. Relatório Técnico. Instituto da Água (INAG). Inédito.
- Monteiro JP, Ribeiro L, Reis E, et al (2007b) Modelling stream-groundwater interactions in the Querença-Silves aquifer system. In: XXXV AIH Congress, Groundwater and Ecosystems. Lisbon, p 10.

- Nicolau R (2002) Modelação e mapeamento da distribuição espacial da precipitação – Uma aplicação a Portugal Continental (Modeling and mapping of the spatial distribution of rainfall). Ph.D. thesis, Universidade Nova de Lisboa, Lisbon.
- Nunes G, Monteiro JP, Martins J (2006) Quantificação do consumo de água subterrânea na agricultura por métodos indirectos (Quantifying groundwater use in agriculture by indirect methods). In: IX Encontro de Utilizadores de Informação Geográfica. Oeiras, pp 15–17.
- Oliveira L, Leitao T, Lobo-Ferreira JP, et al (2011) Água, Ecossistemas Aquáticos e Actividade Humana – Projecto PROWATERMAN. Terceiro Relatório Temático – Resultados Quantitativos e Qualitativos das Campanhas de 2011 e Balanços Hídricos. Referência do Projecto n.º PTDC/AACAMB/105061/2008, 2011.
- Oliveira MM (2004) Recarga de águas subterrâneas: Métodos de avaliação. PhD Thesis, University of Lisbon, Faculty of Sciences, Geology Department, Lisbon.
- Oliveira MM, Oliveira L, Lobo-Ferreira JP (2008) Estimativa da recarga natural no sistema aquífero de Querença-Silves (Algarve) pela aplicação do modelo BALSEQ\_MOD. In: 9.º Congresso da Água - Água: desafios de hoje, exigências de amanhã, Cascais (Portugal), 2 - 4 Abril.
- Ramos, C., Carbonell, E. (1991) Nitrate leaching and soil moisture prediction with the LEACHM model. *Fertilizer Research* 27, 171-180p.
- Šimůnek, J., Šejna, M., Saito, H., Sakai, M., van Genuchten, M. (2013) The HYDRUS 1.D Software Package for Simulating the One-Dimensional Movement of Water, Heat, and Multiple Solutes in Variably-Saturated Media – Version 4.17. Department of Environmental Sciences, University of California, 308pp.
- Stigter T, Dill A, Malta E, Santos R (2013) Nutrient sources for green macroalgae in the Ria Formosa lagoon - assessing the role of groundwater. In: *Groundwater and Ecosystems*. CRC Press, pp 153–167.
- Stigter T, Ribeiro L, Dill AC, Reis E (2006a) Caracterização Do Actual Estado De Aplicação Da Directiva Nitratos 91/676/ Cee No Algarve. 8º Congr da Água 16.
- Stigter TY, Carvalho Dill a. MM, Ribeiro L, Reis E (2006b) Impact of the shift from groundwater to surface water irrigation on aquifer dynamics and hydrochemistry in a semi-arid region in the south of Portugal. *Agric Water Manag* 85:121–132. doi: 10.1016/j.agwat.2006.04.004.
- Stigter TY, Monteiro JP, Nunes LM, et al (2009) Screening of sustainable groundwater sources for integration into a regional drought-prone water supply system. *Hydrol Earth Syst Sci Discuss* 6:85–120. doi: 10.5194/hessd-6-85-2009.
- Stigter TY, Ribeiro L, Dill a. MMC (2008) Building factorial regression models to explain and predict nitrate concentrations in groundwater under agricultural land. *J Hydrol* 357:42–56. doi: 10.1016/j.jhydrol.2008.05.009.